Non-equilibrium and local detection of the normal fraction of a trapped two-dimensional Bose gas

Iacopo Carusotto, Yvan Castin

Non-equilibrium and local detection of the normal fraction of a trapped two-dimensional Bose gas

Iacopo Carusotto[1] and Yvan Castin[2]

[1]*INO-CNR BEC Center and Dipartimento di Fisica, Università di Trento, I-38123 Povo, Italy*
[2]*Laboratoire Kastler Brossel, École normale supérieure, UPMC and CNRS, 24 rue Lhomond, 75231 Paris Cedex 05, France*

We propose a method to measure the normal fraction of a two-dimensional Bose gas, a quantity that generally differs from the Bose-Einstein condensed fraction. The idea is based on applying a spatially oscillating artificial gauge field to the atoms. The response of the atoms to the gauge field can be read out either mechanically from the deposited energy into the cloud, or optically from the macroscopic optical properties of the atomic gas. The local nature of the proposed scheme allows one to reconstruct the spatial profile of the superfluid component; furthermode, the proposed method does not require having established a thermal equilibrium condition in the gas in the presence of the gauge field. The theoretical description of the system is based on a generalization of the Dum-Olshanii theory of artificial gauge fields to the many-body context. The efficiency of the proposed measurement scheme is assessed by means of classical field numerical simulations. An explicit atomic level scheme minimizing disturbing effects such as spontaneous emission is proposed for ^{87}Rb atoms.

PACS numbers: 67.85.-d, 47.37.+q, 37.10.Vz, 42.50.Gy,

I. INTRODUCTION

One of the most striking features of degenerate Bose gases in two dimensions is the possibility of having a superfluid behavior in the absence of a macroscopically populated Bose-Einstein condensate. The transition to the superfluid state is of the Berezinskii-Kosterlitz-Thouless type, characterized by a sudden jump of the superfluid density from 0 to the universal value 4 (in units of the inverse square of the de Broglie thermal wavelength), independent from the details of the system [1, 2]. At the transition point, the asymptotic behavior of the field correlation function changes from an exponential to a power-law decay at large distances. In contrast to the three-dimensional case, superfluidity is then not related to the appearance of a macroscopically occupied Bose-Einstein condensate in the thermodynamic limit.

Pioneering experiments have addressed the mechanical properties of two-dimensional layers of liquid Helium adsorbed on a substrate [3] and have characterized the universal jump of the superfluid fraction at the Berezinskii-Kosterlitz-Thouless critical point. On the other hand, liquid Helium experiments have limited access to the momentum distribution and the correlation functions of the fluid. The situation of ultracold atom experiments is almost the opposite: evidence of the BKT transition has been obtained from the coherence functions [4], the number of observed vortices [5], and the density profile after time-of-flight [6], while the macroscopic mechanical properties of the fluid have not been characterized yet.

Quite some effort has been recently devoted to the conceptual problem of how to experimentally detect genuine superfluidity in a quantum gas of ultracold atoms and not simply Bose-Einstein condensation [7]. A possibility explored in [8] is to look at the response of a gas in a toroidal trap to a static azimuthal artificial gauge field: a spectroscopic signature is proposed which should provide direct information on the total superfluid mass of the system. A different strategy proposed in [9] consists of looking at the evolution of the density profile of a trapped gas when this is set into rotation.

In the present paper we propose two experimental protocols to measure the superfluid fraction of a gas in a *local* way, so to extract its spatial dependence in a trapped geometry. This feature is most relevant for atomic samples, as the superfluid core co-exists with an external ring of normal gas [10]. In particular, the proposed diagnostic technique does not require to relate experimental observations after time of flight to in-trap quantities. Furthermore, in contrast to [9] our technique does not require thermodynamic equilibrium in the gas in presence of rotation [53] and may be applied to more general, non-equilibrium conditions.

The basic idea of our proposal is based on the definition of normal and superfluid fractions of a quantum fluid in terms of its current response to a transverse gauge field in the low-frequency and long-wavelength limit [14, 15]. A spatially oscillating artificial gauge field [16, 17, 20, 21] with a spatially localized envelope can be applied to the atomic gas using a suitable combination of laser beams. The response of the fluid to the gauge field can be detected either mechanically or optically. In the former case, one has to measure the amount of energy that is deposited in the atomic gas at the end of a suitable temporal sequence of gauge field. In the latter case, one can observe e.g. the phase shift that is experienced by the laser fields while crossing the atomic cloud.

The structure of the paper is as follows. In Sec.II we review the definition of the normal and superfluid fractions that we adopt throughout the whole paper. The strategy to generate the artificial gauge field with the suitable spatial geometry is presented in Sec.III. The first method to mechanically measure the normal fraction by detecting the deposited energy at the end of a suitable temporal

sequence of gauge field is discussed in Sec.IV: after presenting the general idea, the efficiency of the method is validated on classical field numerical simulations. The second, all-optical method is presented in Sec.V. A rigorous derivation of the optical polarization of the atomic cloud under the effect of the laser beams is presented and applied to our geometry. Clear signatures of superfluidity are identified in the macroscopic transmission and scattering properties of the atomic cloud. Conclusions are drawn in Sec.VI. The Appendices provide more details on the calculations as well as some realistic estimates for ^{87}Rb atoms in a specific, most promising configuration of atomic levels and laser fields.

II. PRINCIPLE OF THE METHOD

Our proposal to quantitatively assess the superfluidity of the two-dimensional atomic gas is based on the traditional definition of the normal fraction f_n in terms of the response to a transverse gauge field coupling to the atomic current operator [14, 15]. The interaction Hamiltonian has the form:

$$V = -\int d^2\mathbf{r}\, \mathbf{A}(\mathbf{r}) \cdot \mathbf{j}(\mathbf{r}) \tag{1}$$

with the current operator defined as usual as

$$\mathbf{j}(\mathbf{r}) = \frac{\hbar}{2im}\left[\hat{\phi}^\dagger(\mathbf{r})\nabla\hat{\phi}(\mathbf{r}) - \text{h.c.}\right] \tag{2}$$

in terms of the bosonic field operator $\hat{\phi}$ for the two-dimensional gas. For a spatially homogeneous system, the linear response susceptibility relating the average current [54] to the applied gauge field can be easily written in momentum space as

$$\langle \mathbf{j} \rangle(\mathbf{q},\omega) = \chi(\mathbf{q},\omega)\, \mathbf{A}(\mathbf{q},\omega). \tag{3}$$

If the system is also invariant under reflection with respect to the direction of $\mathbf{q}$, the susceptibility tensor $\chi(\mathbf{q},\omega)$ turns out to be diagonal in the longitudinal/transverse basis with respect to $\mathbf{q}$, with elements $\chi_{L,T}(\mathbf{q},\omega)$, respectively.

For a system of density ρ, the normal fraction f_n of the system is then defined as the low-momentum, low-frequency limit of the susceptibility to transverse gauge fields:

$$f_n = \lim_{q\to 0}\lim_{\omega\to 0} \frac{m}{\rho}\chi_T(\mathbf{q},\omega). \tag{4}$$

Note that the order of the limits is here important. A well-known sum rule based on gauge invariance imposes that the same limit for the longitudinal susceptibility $\chi_L(\mathbf{q},\omega)$ gives exactly unity,

$$1 = \lim_{q\to 0}\lim_{\omega\to 0} \frac{m}{\rho}\chi_L(\mathbf{q},\omega). \tag{5}$$

The definition (4) can then be extended to large but finite systems using the standard local density approximation.

In what follows we will propose two methods to exploit the definition (4). The first method is an all-mechanical one, where one measures the deposited energy after a suitable excitation sequence by a spatially modulated gauge field. The second method is based on the optical detection of the current induced by the gauge field.

III. HOW TO GENERATE THE GAUGE FIELD

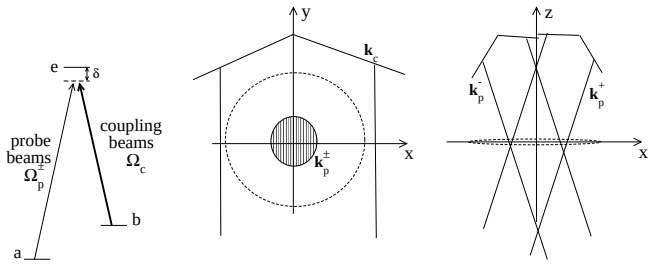

FIG. 1: Scheme of the set-up under consideration. Left panel: generic sketch of the Λ configuration of atomic levels and laser beams involved in the optical processes. Center panel: view from above of the two-dimensional atomic pancake and of the laser beams. Right panel: side view. $\mathbf{k}_c$ and $\mathbf{k}_p^\pm$ are the wavevectors of the coupling and probe beams, respectively. In practice, $\mathbf{k}_p^\pm = (k_p^2 - q^2/4)^{1/2}\,\mathbf{e}_z \pm (q/2)\,\mathbf{e}_x$ with $q \ll k_p$.

We consider a three-dimensional gas of bosonic atoms in a strongly anisotropic, pancake-shaped trap. The axial confinement frequency ω_z is much higher than the one $\omega_\parallel$ along the xy plane; both the temperature T (times the Boltzmann constant k_B) and the chemical potential μ of the gas are assumed to be smaller than $\hbar\omega_z$. In this regime, the gas will be eventually described in terms of a two-dimensional Hamiltonian.

Building on an idea originally introduced in [16], an artificial gauge field coupling to the atomic current can be obtained by illuminating the atoms with several laser beams with suitably chosen frequencies, wavevectors, and waist profiles. Several schemes to generate artificial gauge fields for neutral atoms have been proposed in the last years [16, 17, 20]. The last proposal [20] was recently implemented on an atomic Bose-Einstein condensate: for sufficiently strong gauge fields, a disordered ensemble of vortices appeared in the gas [21].

In the present paper, we shall focus our attention on the level configuration shown in Fig.1. Three internal atomic levels in a Λ configuration are connected by three laser fields according to the sketch given in the left panel of Fig.1: a coupling beam resonantly drives the $b \to e$ atomic transition, while a pair of probe beams resonantly drive the $a \to e$ one. The artificial gauge field originates from the spatial and temporal dependence of the optically dark state. All other atomic states are assumed to be far-off resonance; a complete discussion of their effect in the

specific case of ^{87}Rb atoms will be given in Appendix A.

The geometrical arrangement of the laser beams is sketched in the center and right panels of Fig.1. The continuous-wave control c beam propagates along the y direction with a wavevector $\mathbf{k}_c$ and a frequency ω_c close to resonance with the $b \to e$ transition, and has a peak Rabi frequency Ω_c^o. Its waist profile is much wider than the size of the atomic cloud, so that it can be safely approximated by a plane wave.

The two probe beams share the same carrier frequency ω_p close to resonance with the $a \to e$ transition. The frequencies of the coupling and probe beams are chosen exactly on resonance with the Raman transition $a \to e \to b$, $\omega_p - \omega_c = \omega_b - \omega_a$. The probe beams impinge on the atomic cloud with wavevectors $\mathbf{k}_p^{\pm} \simeq k_p \mathbf{e}_z \pm \mathbf{q}/2$ close to the z direction and symmetrically located with respect to it. The difference $\mathbf{q} = \mathbf{k}_p^+ - \mathbf{k}_p^-$ lies along the xy plane and is in magnitude $q \ll k_p = \omega_p/c$. Their spatial profile is taken to be a Gaussian, centered at $\mathbf{r}_0$ in the $z = 0$ plane, with a waist w.

In what follows, we shall always assume that $w \gg q^{-1}$, so to ensure that the volume of the gas within the waist is "macroscopic": in this way, the relation Eq.(4) for the normal fraction can be used. At the same time, the waist w is assumed to be much smaller than the atomic cloud radius, so to allow for a local measurement of the normal fraction. The peak Rabi frequencies of the two probe beams are $\Omega_p^{\pm}(t)$, respectively (see Appendix B for the definition of the Rabi frequencies). The spatial dependence of the Rabi frequencies of both the coupling and the probe beams is then summarized by the following expressions [55],

$$\Omega_c(\mathbf{r},t) = \Omega_c^0 e^{-i\Delta_c t}\, e^{i\mathbf{k}_c\cdot\mathbf{r}} \tag{6}$$

$$\Omega_p(\mathbf{r},t) \simeq [\Omega_p^+\, e^{i\mathbf{k}_p^+\cdot\mathbf{r}} + \Omega_p^-\, e^{i\mathbf{k}_p^-\cdot\mathbf{r}}] \times e^{-[(x-x_0)^2+(y-y_0)^2]/w^2}. \tag{7}$$

where we have allowed for the coupling beam to have a small detuning Δ_c from Raman resonance on top of its carrier frequency at ω_c. On the contrary, Ω_p does not have a time dependent phase factor, but only contains a purely real non-negative switch-on and switch-off function $f(t)$,

$$\Omega_p(\mathbf{r},t) = \Omega_p^0(\mathbf{r})[f(t)]^{1/2}. \tag{8}$$

In what follows, we shall restrict our attention to the non-saturating regime $|\Omega_c|, |\Omega_p^{\pm}| \ll |\delta + i\Gamma/2|$, where Γ is the decay rate of $|e\rangle$ due to spontaneous emission, and δ is the common detuning of the probe and control beam carrier frequencies from the transitions $|a\rangle \to |e\rangle$ and $|b\rangle \to |e\rangle$ respectively. We shall also concentrate on the limit $|\Omega_p^{\pm}| \ll |\Omega_c|$ where the structure of the gauge field is the simplest.

As the transitions driven by the probe and control beams share the excited state, for each spatial and temporal position $(\mathbf{r},t)$ an internal *non-coupled state* exists for which the two excitation channels interfere destructively. In terms of the local Rabi frequencies $\Omega_p(\mathbf{r},t)$ and $\Omega_c(\mathbf{r},t)$, this non-coupled state reads

$$|NC(\mathbf{r},t)\rangle = \frac{|a\rangle - \Omega_p(\mathbf{r},t)/\Omega_c(\mathbf{r},t)\,|b\rangle}{(1+|\Omega_p(\mathbf{r},t)|^2/|\Omega_c(\mathbf{r},t)|^2)^{1/2}}. \tag{9}$$

Eliminating the excited state $|e\rangle$, one sees that the bright orthogonal state, the so-called coupled state,

$$|C(\mathbf{r},t)\rangle = \frac{[\Omega_p(\mathbf{r},t)/\Omega_c(\mathbf{r},t)]^*|a\rangle + |b\rangle}{(1+|\Omega_p(\mathbf{r},t)|^2/|\Omega_c(\mathbf{r},t)|^2)^{1/2}} \tag{10}$$

is separated from $|NC(\mathbf{r},t)\rangle$ by a (complex) energy gap

$$\hbar[\delta'(\mathbf{r},t) - i\Gamma'(\mathbf{r},t)/2] \equiv \frac{\hbar[|\Omega_c(\mathbf{r},t)|^2 + |\Omega_p(\mathbf{r},t)|^2]}{4(\delta + i\Gamma/2)}, \tag{11}$$

where δ' and Γ' are the lightshift and the decay rate of the coupled state. If the energy gap is large enough as compared to both the motional coupling between $|NC\rangle$ and $|C\rangle$ due to the spatio-temporal dependence of Ω_c and $\Omega_p^{\pm}$, and to the quantum of oscillation $\hbar\omega_z$ along the tightly confined z direction, we can restrict the dynamics to the $|NC\rangle$ internal state.

Generalizing the single-particle theory of [16] to the many-body context, one gets to an effective Hamiltonian for the component $\hat{\phi}_{3D}(\mathbf{r},t)$ of the three-dimensional atomic field operator in the (spatially and temporally-dependent) non-coupled state $|NC\rangle$,

$$\hat{\phi}_{3D}(\mathbf{r},t) = \langle NC(\mathbf{r},t)|a\rangle\, \hat{\Psi}_a(\mathbf{r},t) + \langle NC(\mathbf{r},t)|b\rangle\, \hat{\Psi}_b(\mathbf{r},t) \tag{12}$$

in the simple form [56]:

$$\mathcal{H} = \int d^3\mathbf{r}\, \left\{ \hat{\phi}_{3D}^\dagger \left[-\frac{\hbar^2\nabla^2}{2m} + U(\mathbf{r}) + W_{3D}(\mathbf{r},t) \right] \hat{\phi}_{3D} - \mathbf{j}_{3D}(\mathbf{r})\cdot\mathbf{A}_{3D}(\mathbf{r},t) + \frac{1}{2} g(\mathbf{r},t)\, \hat{\phi}_{3D}^\dagger \hat{\phi}_{3D}^\dagger \hat{\phi}_{3D} \hat{\phi}_{3D} \right\} \tag{13}$$

where the vector gauge potential

$$\mathbf{A}_{3D}(\mathbf{r},t) = \frac{i\hbar}{2} \Big[\langle NC(\mathbf{r},t)[\nabla|NC(\mathbf{r},t)\rangle] - \text{c.c.} \Big] \tag{14}$$

couples to the atomic current operator

$$\mathbf{j}_{3D}(\mathbf{r}) = \frac{\hbar}{2im} \left[\hat{\phi}_{3D}^\dagger(\mathbf{r}) \nabla \hat{\phi}_{3D}(\mathbf{r}) - \text{h.c.} \right]. \tag{15}$$

and the scalar potential

$$W_{3D}(\mathbf{r},t) = -\frac{i\hbar}{2} \Big[\langle NC(\mathbf{r},t)\, [\partial_t|NC(\mathbf{r},t)\rangle] - \text{c.c.} \Big] + + \frac{\hbar^2}{2m} \sum_{i=x,y,z} [\partial_{r_i}\langle NC(\mathbf{r},t)]|[\partial_{r_i}|NC(\mathbf{r},t)\rangle] \tag{16}$$

couples to the density

$$n_{3D}(\mathbf{r}) = \hat{\phi}_{3D}^\dagger(\mathbf{r})\, \hat{\phi}_{3D}(\mathbf{r}). \tag{17}$$

The derivation of the Hamiltonian (13) is based on the Quantum Stochastic Differential Equations formalism [25]; the details are given in the Appendix B.

The spatial and temporal dependence of the a, b weights of the non-coupled state (9) reflects into a similar variation of the coupling constant describing the atomic interaction within the internal state $|NC\rangle$:

$$g_{3D}(\mathbf{r}) = \frac{|\Omega_c|^4 g_{aa} + 2|\Omega_p(\mathbf{r})|^2 |\Omega_c|^2 g_{ab} + |\Omega_p|^4 g_{bb}}{(|\Omega_c|^2 + |\Omega_p(\mathbf{r})|^2)^2}, \tag{18}$$

where the coupling constants g_{aa}, g_{ab} and g_{bb} originate from the $a-a$, $a-b$ and $b-b$ elastic s-wave interactions. In what follows, we shall be interested in isolating the response of the system to the gauge field $\mathbf{A}$. To this purpose, it will be useful to minimize the effect of all unwanted couplings to the density introduced by the scalar potential W_{3D} and by the spatial dependence of the interaction constant g_{3D}. This latter effect is minimized if one chooses states a, b with similar scattering properties $g_{aa} \simeq g_{ab} \simeq g_{bb}$. In the limit $|\Omega_p/\Omega_c| \ll 1$, one simply needs to have $g_{aa} \simeq g_{ab}$, as it is assumed from now on.

The atomic wavefunction along z is assumed to be frozen in the ground state of the harmonic confinement of wavefunction $\phi_0(z)$. This allows to express the three-dimensional bosonic field $\hat{\phi}_{3D}$ in terms of the bosonic field for a two-dimensional gas, setting

$$\hat{\phi}_{3D}(x, y, z) = \phi_0(z)\hat{\phi}(x, y). \tag{19}$$

Correspondingly, the two-dimensional coupling constant g has the expression

$$g = \frac{\hbar^2}{m}\tilde{g} = \frac{g_{3D}}{\sqrt{2\pi}\, a_{ho}} \tag{20}$$

in terms of the three-dimensional coupling constant g_{3D} and the size $a_{\rm ho}^z = \sqrt{\hbar/m\omega_z}$ of the ground state along z. Note that the dimensional reduction (19) does not require being in the Lamb-Dicke limit $k_{p,c}a_{\rm ho}^z \ll 1$.

The effective two-dimensional gauge and scalar potentials $\mathbf{A}$ and W then result from an average of the Hamiltonian (13) over the motional ground state along z. Including in (14) and (16) the explicit form of the beam profiles and restricting ourselves to zeroth order in the small parameters $q/k_{p,c}$, $1/wk_{p,c}$, and to second order in $\Omega_p^{\pm}/\Omega_c$, the resulting two-dimensional gauge potential turns out to be directed along the y axis and have the form

$$\begin{aligned} A_y(\mathbf{r}) &\simeq \hbar k_c \frac{\left|\Omega_p^+ e^{i\mathbf{q}\cdot\mathbf{r}/2} + \Omega_p^- e^{-i\mathbf{q}\cdot\mathbf{r}/2}\right|^2}{|\Omega_c|^2} e^{-2|\mathbf{r}-\mathbf{r}_0|^2/w^2} \\ &= \hbar k_c \frac{|\Omega_p^+|^2 + |\Omega_p^-|^2 + [\Omega_p^+\Omega_p^{-*} e^{i\mathbf{q}\cdot\mathbf{r}} + \text{c.c.}]}{|\Omega_c|^2} \\ &\qquad \times e^{-2|\mathbf{r}-\mathbf{r}_0|^2/w^2}. \end{aligned} \tag{21}$$

To the same level of approximation, the scalar potential has the form

$$\begin{aligned} W(\mathbf{r}) = &\left[\frac{\hbar^2(k_c^2 + k_p^2)}{2m} + \hbar\Delta_c\right] \\ &\times \frac{\left|\Omega_p^+ e^{i\mathbf{q}\cdot\mathbf{r}/2} + \Omega_p^- e^{-i\mathbf{q}\cdot\mathbf{r}/2}\right|^2}{|\Omega_c|^2} e^{-2|\mathbf{r}-\mathbf{r}_0|^2/w^2}, \end{aligned} \tag{22}$$

which can be made to vanish by choosing a detuning Δ_c that exactly compensates the recoil of the atoms after the Raman process $a \to e \to b$:

$$W \equiv 0 \quad \text{for} \quad \Delta_c = -\frac{\hbar(k_c^2 + k_p^2)}{2m}. \tag{23}$$

It is worth pointing out that the real switch-on and switch-off function $f(t)$ of the probe beam Eq.(8) has an exactly vanishing contribution to the temporal derivative term in the right-hand side of Eq.(16) [57].

After expansion of the squared modulus as done in the second line of (21), two kinds of terms are immediately identified: (i) a slowly varying Gaussian term of size w and peak amplitude $|\Omega_p^+|^2 + |\Omega_p^-|^2$ that follows the laser envelopes, and (ii) an oscillating term at wavevector $\mathbf{q}$ with a Gaussian envelope of size w and peak amplitude $|\Omega_p^+\Omega_p^-|$. This spatially modulated term is indeed the one that we need to probe the normal fraction of the gas according to the definition (4): when $\mathbf{q}$ is taken along the x axis (y axis), it provides an almost purely transverse (longitudinal) contribution to the gauge field $\mathbf{A}$. On the other hand, the slowly varying term always includes both longitudinal and transverse vector field components. Experimental procedures to subtract the effect of this unwanted term will be discussed in the next sections.

IV. DEPOSITED ENERGY MEASUREMENT

A. General idea

In this section we shall present a method to extract the value of the normal fraction from a measurement of the energy that is deposited in the system by a suitably designed gauge field sequence. The coupling beam is assumed to be always on. On the other hand, both probe beam intensities $|\Omega_p^{\pm}|^2$ are varied in time according to the (dimensionless) real envelope function $f(t)$. This is chosen to be 0 for $t < 0$ and to rapidly tend back to 0 at long times.

As already mentioned, we assume that the atomic interaction constants satisfy $g_{aa} \simeq g_{ab}$ [58]. As soon as $qw \gg 1$, the deposited energy is the sum of two independent contributions $\Delta E_{1,2}$ corresponding to the decomposition (21) of the gauge field as the sum of a non-modulated term and a modulated one at the wavevector $\mathbf{q}$. Using standard linear response theory within the local density approximation as discussed in the Appendix C, the contribution ΔE_2 of the modulated term can be

written in the simplified form

$$\Delta E_2 \simeq \frac{\pi}{4} w^2 \left(\frac{\epsilon_{\rm gauge}}{2}\right)^2 \int_{-\infty}^{+\infty} \frac{d\omega}{\pi}\, \omega\, |f(\omega)|^2\, {\rm Im}[\chi_{yy}(\mathbf{q},\omega)] \tag{24}$$

where we have introduced the amplitude of the spatially modulated part of the gauge field,

$$\epsilon_{\rm gauge} = 2\,\hbar k_c\, \frac{|\Omega_p^+\,\Omega_p^-|(t=0^+)}{|\Omega_c|^2}. \tag{25}$$

A similar expression for the contribution ΔE_1 of the non-modulated term is given in the Appendix C as (C8).

The expression (24) for the deposited energy involves the imaginary part of the susceptibility, while the normal fraction (4) involves the real part. To relate the two, one can make use of the well-known Kramers-Kronig relation of linear response theory,

$$\lim_{\omega\to 0} {\rm Re}[\chi(\mathbf{q},\omega)] = \int_{-\infty}^{+\infty} \frac{d\omega'}{\pi}\, \frac{{\rm Im}[\chi(\mathbf{q},\omega')]}{\omega'}. \tag{26}$$

For a suitably chosen envelope of the form $f(t) = e^{-\gamma t}\,\Theta(t)$, whose Fourier transform has the form $f(\omega) = i/(\omega + i\gamma)$, the integral in (24) indeed reduces to the real part of the susceptibility (26) in the $\gamma \to 0$ limit.

As a consequence, the deposited energy ΔE_2 for small $\mathbf{q}$ perpendicular (parallel) to $\mathbf{k}_c$ can be related to the normal (total) density ρ_n (ρ) at position $\mathbf{r}_0$ by

$$\Delta E_2 \simeq \frac{\pi}{4}\frac{w^2}{m} \left(\frac{\epsilon_{\rm gauge}}{2}\right)^2 \times \begin{cases} \rho_n(\mathbf{r}_0) & \text{for } \mathbf{q} \perp \mathbf{k}_c \\ \rho(\mathbf{r}_0) & \text{for } \mathbf{q} \parallel \mathbf{k}_c \end{cases}. \tag{27}$$

For intermediate angles α between $\mathbf{q}$ and $\mathbf{k}_c$, δE_2 is proportional to $\cos^2\alpha\,\rho + \sin^2\alpha\,\rho_n$ [27].

In an actual experiment, the undesired contribution ΔE_1 can be eliminated by noting its independence on the relative orientation of $\mathbf{q}$ and $\mathbf{k}_c$ [see Eqs.(C8) and (C9)], as well as its different dependence on the probe amplitudes $\Omega_p^\pm$, proportional to $[|\Omega_p^+|^2 + |\Omega_p^-|^2]^2$ rather than $|\Omega_p^+\Omega_p^-|^2$. By measuring the deposited energy for at least two different values of the Ω_p^+/Ω_p^- ratio, one is able to isolate the relevant contribution (27).

B. How fast is the $q, \gamma \to 0$ limit reached ?

An important point in view of experiments is to characterize how small q and γ have actually to be taken to obtain a quantitatively accurate measurement of the normal fraction f_n. To answer this question, we consider in this subsection the simplest case of a spatially homogeneous system in a square box of size L with periodic boundary conditions, excited by a gauge field in a plane wave form, i.e. in the limit $w \to \infty$. We also limit ourselves to the case of a transverse gauge field with $\mathbf{q} = q\,\mathbf{e}_x$ perpendicular to $\mathbf{k}_c = k_c\,\mathbf{e}_y$,

$$\mathbf{A}_{\rm ideal}(\mathbf{r},t) = \Theta(t) e^{-\gamma t} \mathbf{e}_y \frac{\epsilon_{\rm gauge}}{2} \left(e^{iqx} + e^{-iqx}\right). \tag{28}$$

The deposited energy at the end of the gauge field sequence can be evaluated by means of the Bogoliubov theory of dilute Bose gases. The main steps of the calculation are sketched in Appendix D. The final result reads

$$\Delta E_2 = \left(\frac{\epsilon_{\rm gauge}}{2}\right)^2 \frac{N}{m}\, f_n^{\rm eff} \tag{29}$$

in terms of the wavevector- and γ-dependent effective normal fraction $f_{\rm eff}^n$

$$\begin{aligned} f_n^{\rm eff} = \frac{1}{N} \sum_{\mathbf{k}\neq\mathbf{0},-\mathbf{q}} \frac{\hbar^2 k_y^2}{m} \times \\ {\rm Re}\Big[\frac{n_{\mathbf{k}} - n_{\mathbf{k}+\mathbf{q}}}{\epsilon_{\mathbf{k}+\mathbf{q}} - \epsilon_{\mathbf{k}} - i\hbar\gamma} \left(U_{\mathbf{k}} U_{\mathbf{k}+\mathbf{q}} - V_{\mathbf{k}} V_{\mathbf{k}+\mathbf{q}}\right)^2 \\ + \frac{1 + n_{\mathbf{k}} + n_{\mathbf{k}+\mathbf{q}}}{\epsilon_{\mathbf{k}+\mathbf{q}} + \epsilon_{\mathbf{k}} - i\hbar\gamma} \left(U_{\mathbf{k}} V_{\mathbf{k}+\mathbf{q}} - V_{\mathbf{k}} U_{\mathbf{k}+\mathbf{q}}\right)^2 \Big]. \end{aligned} \tag{30}$$

Here $N = \rho L^2$ is the total particle number,

$$\epsilon_{\mathbf{k}} = \left[\frac{\hbar^2 k^2}{2m}\left(\frac{\hbar^2 k^2}{2m} + 2\rho g\right)\right]^{1/2} \tag{31}$$

is the usual Bogoliubov dispersion relation and the amplitudes of the Bogoliubov modes satisfy

$$U_k + V_k = \frac{1}{U_k - V_k} = \left(\frac{\hbar^2 k^2/2m}{\hbar^2 k^2/2m + 2\rho g}\right)^{1/4} \tag{32}$$

The n_k are the mean occupation number of Bogoliubov modes, $n_k = 1/[\exp(\epsilon_k/k_B T) - 1]$.

The thermodynamic limit $L \to \infty$ at fixed N/L^2 can be worked out analytically by first taking the $\gamma \to 0$ limit and then the $q \to 0$ limit in the expression (30) for $f_n^{\rm eff}$. In this way one recovers the usual Bogoliubov expression for the normal fraction, which in dimension two reads:

$$f_n = \frac{1}{\rho} \int \frac{d^2k}{(2\pi)^2} \frac{\hbar^2 k_y^2}{m} (-\partial_{\epsilon_k} n_k). \tag{33}$$

For a finite size system, the dependence of $f_n^{\rm eff}$ on γ and q is explored in Fig.2. For the smallest non-zero wavevector value allowed by the chosen box, the relative error on $f_n^{\rm eff}$ is already on the order of 10% for $\gamma/c_s q = 0.15$.

Another interesting result of Bogoliubov theory applied to our system is a sufficient condition on the amplitude of the gauge field to be within the linear response regime. To this purpose, we can write the equations of motion for the Bogoliubov mode operators $b_{\mathbf{k}}$ in the interaction picture in the presence of the time-dependent gauge field, and impose that the amplitude change be small as compared to the initial value.

The condition is most stringent for modes such that $\epsilon_{\mathbf{k}} = \epsilon_{\mathbf{k}\pm\mathbf{q}}$, where the real part of the energy denominator can vanish. For the maximal value of k set by the thermal occupation, this leads to the sufficient condition

$$\frac{\epsilon_{\rm gauge}}{(m k_B T_d)^{1/2}} \lesssim \left(\frac{T_d}{T}\right)^{1/2} \frac{2\hbar\gamma}{k_B T_d}, \tag{34}$$

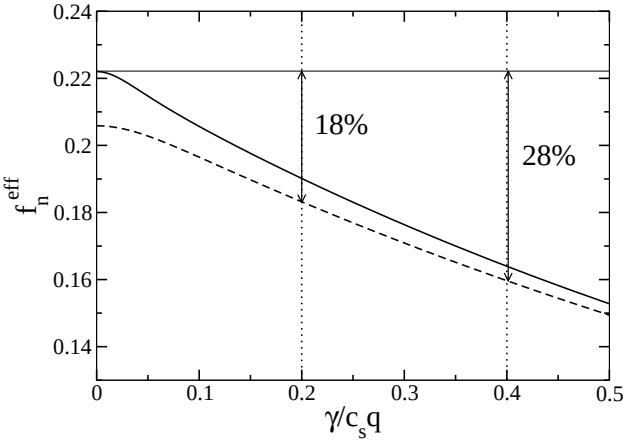

FIG. 2: Bogoliubov prediction (30) for the effective normal fraction $f_n^{\rm eff}$: dependence of $f_n^{\rm eff}$ on γ for two different values of the gauge field wavevector $\mathbf{q} = (2\pi/L)\,\mathbf{e}_x$ (solid, $q\xi \simeq 0.1$) and $\mathbf{q} = 10 \times (2\pi/L)\,\mathbf{e}_x$ (dashed, $q\xi \simeq 1$). System parameters: square box of size $L/\xi \simeq 63$ containing $N \simeq 40000$ particles with interaction constant $g = 0.1\,\hbar^2/m$ at a temperature $T/T_d = 0.1$. $T_d = 2\pi\hbar^2\rho/m$ is the degeneracy temperature. The healing length ξ of the gas is defined by $\hbar^2 m\xi^2 = \rho g$. The dashed line corresponds to the same value of $q\xi \simeq 1$ as in Fig.4 and the vertical dotted lines indicate the values of $\gamma/c_s q$ considered in that figure. The horizontal thin line is the prediction (40) of Bogoliubov theory in the thermodynamic limit [28]. The quadratic rather than linear dependence of $f_n^{\rm eff}$ on γ for small values of γ is a finite-size effect.

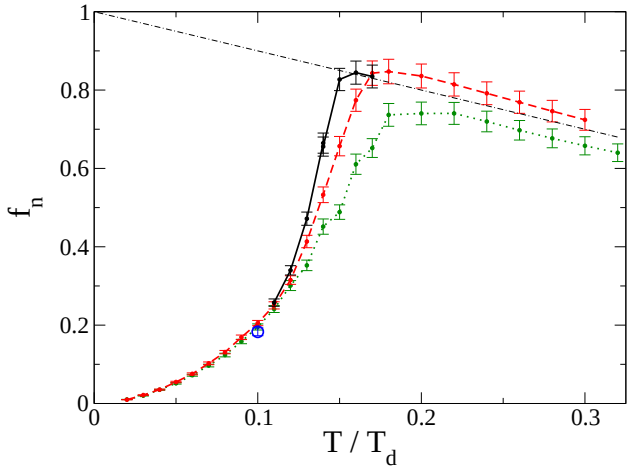

FIG. 3: Classical field simulation of the normal fraction f_n for a two-dimensional, spatially homogeneous interacting Bose gas as a function of temperature. The calculation has been performed using the thermodynamic expression (40) for the normal fraction. The coupling constant is $g = 0.1\,\hbar^2/m$. The different curves refer to simulations performed with different numbers of grid points $M = 16^2$ (green, dotted), 32^2 (red, dashed), 64^2 (black, solid). The number of classical field realizations is $n_{\rm real} = 1000$. The dot-dashed line is the classical field prediction for the normal fraction f_n of an ideal gas in the thermodynamic limit: as discussed in the text, the decrease at high temperatures is an artifact of the classical field model. The blue circle indicates the result of a numerical simulation of the deposited energy scheme as in Fig.4b but for a homogeneous system with an infinite beam waist $w = \infty$, a number of grid points $M = 32^2$, a gauge field wavevector $q = 2\pi/L \simeq 0.2/\xi$, and including a careful extrapolation of $\epsilon_{\rm gauge} \to 0$ (numerics down to $\epsilon_{\rm gauge} = 0.01$) and of $\gamma \to 0$ (numerics down to $\gamma/(c_s q) = 0.05$) extrapolation.

in terms of the degeneracy temperature $k_B T_d = 2\pi\hbar^2\rho m$. This naive argument is however not able to determine to which extent this condition is actually necessary. This would require a higher order calculation which falls beyond the scope of the present work.

C. Numerical investigation

To further assess the validity and accuracy of our proposed scheme we have performed full scale numerical simulations of the response of a two-dimensional Bose gas at finite temperature to the complete gauge field (21), including the Gaussian envelope of the gauge field and a circular well trapping potential. A very useful tool to this purpose is the classical field model developed and applied in a number of recent works [13, 29]. For this model both the thermal equilibrium state and the temporal dynamics can in fact be easily addressed with standard numerical tools and provide reliable results for the physics of the degenerate Bose gas.

We consider a classical **C**-field defined on a square grid. The real space lattice constant b is chosen in terms of the thermal de Broglie wavelength $\lambda = \sqrt{2\pi\hbar^2/mk_BT}$ as $b/\lambda = \sqrt{\pi/4\zeta}$. The value $\zeta \simeq 0.8$ [59] of the numerical coefficient is chosen in such way that the classical field model correctly reproduces the total number of non-condensed particles for an ideal gas at zero chemical potential in the thermodynamic limit. This choice corresponds to setting the ultra-violet momentum cut-off $k_{\rm max} = \pi/b$ at $\hbar^2 k_{\rm max}^2/2m = \zeta k_B T$.

In the grand canonical ensemble, the thermal probability distribution for the interacting classical field follows a Boltzmann $\exp(-E/k_BT)$ law with the Gross-Pitaevskii energy functional [60].

$$E[\Psi] = b^2 \sum_{\mathbf{r}} \Psi^* \left[-\frac{\hbar^2}{2m}\Delta + U(\mathbf{r}) + \frac{g}{2}\,|\Psi|^2 \right] \Psi. \qquad (35)$$

This probability distribution can be sampled by the long time limit of a Ito stochastic differential equation including a drift term and a noise term [30, 31]. The thermal distribution in the canonical ensemble can be sampled by adding projectors to the stochastic differential equation in order to keep the norm constant $\|\Psi\|^2 = N$. This leads

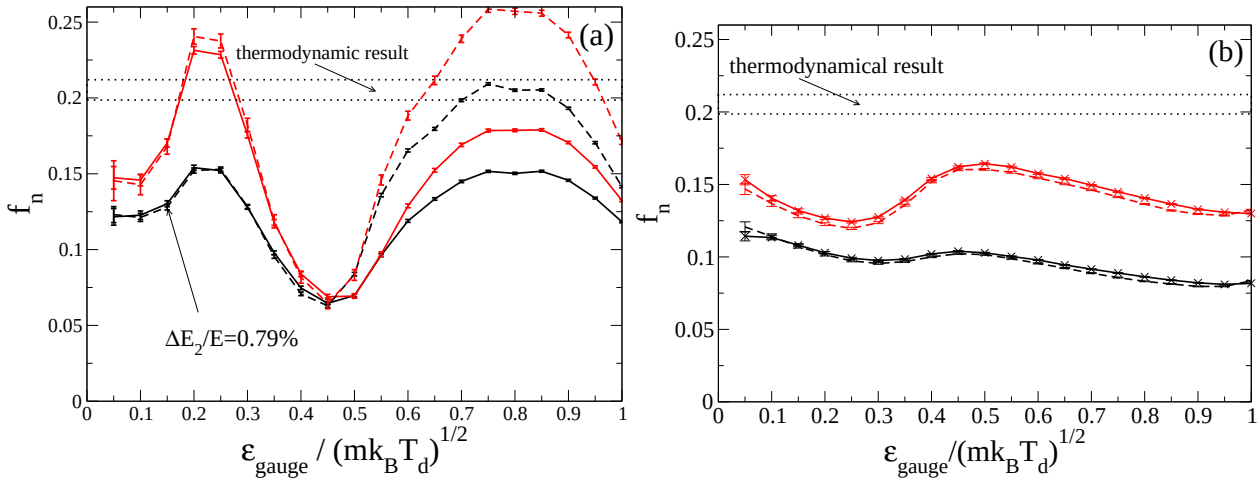

FIG. 4: Classical field simulation of the deposited energy measurement scheme in a realistic geometry. We start from a thermal equilibrium state at $T/T_d = 0.1$ with $g = 0.1\,\hbar^2/m$, and a system size $L/\xi \simeq 63$. Beam waist $w = 30\xi$. Excitation wavevector $q\xi \simeq 1$. The real time evolution is followed up to a time $\tau = 3/\gamma$. The gauge field intensity is measured in terms of $\epsilon_{\rm gauge}$ as defined in (25). In the right (b) panel, only the modulated component is applied. In the left (a) panel, the complete form Eq.(21) is considered, and for each value of $\epsilon_{\rm gauge}$, two calculations are performed to extract the contribution ΔE_2 of the modulated component (see text): the first with $|\Omega_p^+|^2(0^+)/|\Omega_c|^2 = \epsilon_{\rm gauge}/(\hbar k_c)$ and $\Omega_p^- \equiv 0$, the second with $|\Omega_p^\pm|^2(0^+)/|\Omega_c|^2 = \epsilon_{\rm gauge}/(2\hbar k_c)$. Dashed lines correspond to spatially homogeneous system with periodic boundary conditions of side L, which corresponds to $N \simeq 40000$ atoms. Solid lines correspond to the same system in a circular potential well. The total number of atoms is adjusted in a way to have the same central density ρ and hence the same degeneracy temperature T_d and healing length ξ in both cases. Black (red) lines correspond to an excitation sequence with $\gamma/c_s q = 0.4$ ($\gamma/c_s q = 0.2$). Extrapolating linearly to $\gamma = 0$ for the lowest value of the gauge field gives $f_n^{\rm eff} \simeq 0.17$, which is less than 20% away from the actual value. Simulations are performed using 1000 realizations of the classical field. The number of grid points is $M = 64^2$. The region between the horizontal dotted lines indicates the confidence interval of the thermodynamic prediction shown in Fig.3.

to the Ito equation

$$d\Psi = -\frac{1}{2}\,d\tau\,\mathcal{Q}_\Psi\left[-\frac{\hbar^2}{2m}\Delta\Psi + U\,\Psi + g|\Psi|^2\,\Psi\right] + \frac{\sqrt{k_B T}}{b}\,\mathcal{Q}_\Psi d\xi - \frac{M-1}{2N}k_B T\,d\tau\,\Psi. \quad (36)$$

where M is the number of grid points, $\mathcal{Q}_\Psi$ is the projector onto the subspace orthogonal to the classical field Ψ, $d\xi$ is a complex Gaussian, zero-mean, delta-correlated noise such that $d\xi d\xi = 0$ and

$$d\xi^*(\mathbf{r}_i)\,d\xi(\mathbf{r}_j) = d\tau\,\delta_{\mathbf{r}_i,\mathbf{r}_j}. \quad (37)$$

Our numerical procedure consists in first generating a number $n_{\rm real}$ of independent wavefunctions distributed according to the thermal Boltzmann law with energy functional (35) and then to let them evolve in real time according to the time-dependent Gross-Pitaevskii equation including the gauge potential (21).

For the real time evolution, the kinetic, external potential, and interaction energy terms are treated with the usual splitting technique. The evolution operator under the gauge potential (21) during the time-step dt involves numerical evaluation of objects of the form

$$\Psi' = e^{i\lambda(x,t)\,[p_y - h(y))]^2}\,\Psi, \quad (38)$$

where the generic function $h(y)$ has a zero spatial mean over y. This requires a bit more care as the evolution operator is diagonal neither in the real-space nor in the $\mathbf{k}$-space. The trick is to perform a local gauge transform on Ψ of the form

$$U\Psi = e^{-iH(y)/\hbar}\Psi \quad (39)$$

with $dH/dy = h(y)$. In this way, the operator within the exponential in (38) is reduced to a combination of diagonal operators in respectively y and p_y. Since $h(y)$ has a zero mean, $H(0) = H(L)$ and the gauge transform is compatible with the periodic boundary conditions.

As a first application of the classical field method, we have determined the normal fraction of a spatially homogeneous two-dimensional interacting gas at thermal equilibrium. This is done using the thermodynamic formula

$$f_n^{\rm thermo} = \frac{\langle P_y^2\rangle}{N m k_B T} \quad (40)$$

in terms of the thermal variance of the total momentum P_y of the gas [32, 33]. The temperature dependence of the normal fraction is shown in Fig.3 for increasing system sizes. The sudden variation around $T/T_d \simeq 0.13$

becomes sharper and sharper as the system size is increased and should eventually correspond to a discontinuous jump in the superfluid fraction at the BKT transition [1, 2, 34]. The slow decrease for larger values of T/T_d is instead an artifact of the ultraviolet cut-off that has to be imposed to the classical field model in any dimension $d \geq 2$. Indeed, the same decrease is visible also in the case of an ideal gas, for which one can show that $f_n = 1 - T/T_d + O(e^{-T_d/T} T/T_d)$ in the thermodynamic limit.

The experimental estimation of the normal fraction obtained by the deposited energy method discussed in Sec.IV A is simulated in Fig.4. The value of the deposited energy is extracted from the classical field simulation by taking the energy difference at the end of two evolutions from the same initial wavefunction using the same value of $|\Omega_p^+|^2 + |\Omega_p^-|^2$ but different relative magnitudes of $\Omega_p^\pm$. This protocol aims at isolating the effect of the spatially modulated gauge potential: in the linear response limit, it is able to provide the exact value of ΔE_2 alone. The effective normal fraction is then extracted from the deposited energy via (27). In Fig.4, this quantity plotted as a function of the gauge field amplitude for different values of the switch-off rate $\gamma/c_s q = 0.4, 0.2$ (black, red curves) and different geometries (solid, dashed) [61].

The $\epsilon_{\rm gauge}$-dependence allows to estimate the interval where the linear response approximation is reasonable, e.g. for $\epsilon_{\rm gauge}/\sqrt{m k_B T_d} \lesssim 0.15$. As expected, the estimate (34) gives a more pessimistic bound around 0.04. For larger values of the gauge field amplitude $\epsilon_{\rm gauge}$, nonlinear effects set in and the two contributions $\Delta E_{1,2}$ no longer simply add up, which disturbs our protocol to isolate ΔE_1 and introduces spurious corrections to the estimated value of f_n. By comparing the left (a) and right (b) panels of Fig.4 one can see that the marked peaks and the rapid growth for small $\epsilon_{\rm gauge}$ that are visible in (a) are mainly due to a cross-talk effect of the modulated and non-modulated terms. As expected the corresponding curves in the two panels tend to the same value in the small $\epsilon_{\rm gauge}$ limit, which confirms the validity of our protocol to extract ΔE_2. From an experimental point of view, we expect that values of the gauge field amplitude as high as $\epsilon_{\rm gauge}/(\rho k_B T_d)^{1/2} = 0.15$ should be well achievable in practice, see Table I.

For the sake of completeness, it is important to note that for the weak gauge field amplitude that are required to be in the linear regime, the deposited energy ΔE_2 is less than 1% of the total energy of the system, which may be experimentally challenging to measure. This value is however larger than the statistical uncertainty of the energy in the canonical ensemble with $n_{\rm real} = 1000$ realizations. As we shall see better in the next subsection, such a large number of realization turned out necessary in the small $\epsilon_{\rm gauge}$ regime to compensate the fluctuations of the current $\mathbf{j}(t = 0)$ at the initial time.

The residual disagreement of f_n with the thermodynamic result indicated by the dotted lines is of the same order of the finite q and γ correction predicted by Bogoliubov theory, see Fig.2. On a smaller system with $M = 32^2$ modes, we have checked by taking smaller values of q and γ that the thermodynamical prediction is recovered within error bars, see the blue circle in Fig.3. The deviation observed in Fig.4 is therefore not a systematic error of the proposed method.

As a final check, we have validated the locality of the proposed measurement scheme by performing the simulation for two different geometries. Dashed lines in Fig.4 correspond to a spatially homogeneous system with periodic boundary conditions, while the solid lines correspond to a system trapped in a circular well with steep walls of the form $U(\mathbf{r}) = \zeta k_B T \{\tanh[(r - L/2)/(\xi/2)] + 1\}$. The probed region is at the center of the potential well, $r_0 = 0$. Exception made for the strongly nonlinear regime when $\epsilon_{\rm gauge}$ is large, the effective normal fractions are the same in both geometries within error bars.

D. The noise on the deposited energy

In the previous section, while presenting the numerical results, we mentioned the fact that the statistical noise on the deposited energy was larger for smaller values of the gauge field amplitude $\epsilon_{\rm gauge}$.

To understand this feature, it can be useful to rewrite the deposited energy for a single realization of the classical field simulation in the form

$$\delta E = -\int d^2 r\, \mathbf{j}(\mathbf{r}, 0) \cdot \mathbf{A}(\mathbf{r}, 0^+) - \int_{0^+}^{+\infty} dt \int d^2 r\, \mathbf{j}(\mathbf{r}, t)\, \partial_t \mathbf{A}(\mathbf{r}, t). \quad (41)$$

The first term comes from the abrupt switch-on of the gauge field. For each realization, it is of order $\epsilon_{\rm gauge}$ but averages to zero in the limit of an infinite number of realizations of the experiment as $\langle \mathbf{j}(\mathbf{r}, 0) \rangle = 0$. In any actual calculation, an average over a finite number $n_{\rm real}$ of realizations is taken, which gives a non-zero random value scaling as $\epsilon_{\rm gauge}/\sqrt{n_{\rm real}}$.

The relevant signal $\langle \delta E \rangle$ is given by the second term, obtained from the classical Hamiltonian identity $dH/dt = \partial_t H$. For small values of γ, this term is of order $O(\epsilon_{\rm gauge}^2)$ as in this limit $\mathbf{j}$ adiabatically follows the thermal equilibrium value for the instantaneous value of the gauge field. As a result, the number of realizations that are needed to extract the signal out of the statistical noise due to the first term grows as $|\epsilon_{\rm gauge}|^{-2}$, which perfectly explains the numerical observation.

However, it has been demonstrated by a number of recent cold atom experiments that noise is not always just an hindrance but can be also a source of useful physical information [35, 36]. As a simple example, we consider here the amplitude of the noise on the energy that is deposited in the system at each realization of the experiment. This quantity is quantified by the average $\langle \delta E^2 \rangle$ of the square of the deposited energy in the $\gamma \to 0$ limit.

Looking at (41), it is immediate to see that in the small $\epsilon_{\rm gauge}$ limit the dominant contribution comes from the square of the first term, which suggests that the noise on the deposited energy is related to the variance of the instantaneous fluctuations of the current operator. From the fluctuation-dissipation theorem, this quantity can then be related to the normal fraction of the gas.

This idea can be put on solid grounds by developing a full quantum calculation. The linear response theory calculation performed along the lines of Appendix D leads to the expression in Heisenberg picture

$$\lim_{\gamma\to 0}\langle[H_0(+\infty)-H_0(0)]^2\rangle \simeq \langle[\int d^2r\,\mathbf{j}(\mathbf{r})\cdot\mathbf{A}(\mathbf{r},0^+)]^2\rangle \quad (42)$$

where H_0 is the unperturbed Hamiltonian. This relation connects the variance of the quantum equivalent of the deposited energy to the instantaneous fluctuations of the current operator and confirms our expectation based on the classical field model.

In view of experiments, it is however crucial to note that the definition of the deposited energy adopted in (42) involves taking expectation values of the Hamiltonian operator at different times. This may be experimentally challenging as it requires either a non-destructive measurement of the initial energy of the system at $t = 0$ before switching on the gauge field, or a very precise *a priori* knowledge of its value in a sort of microcanonical ensemble [62].

For a generic hermitian operator V with vanishing diagonal matrix elements in the eigenbasis of H_0, the fluctuation-dissipation theorem of linear response theory relates the imaginary part of the susceptibility χ to the Fourier transform of the correlation function $S_{VV}(t) = \langle V(t)\,V(0)\rangle$,

$$\mathrm{Im}[\chi_{VV}(\omega)] = \frac{1}{2\hbar}S_{VV}(\omega)\left[1-e^{-\hbar\omega/k_BT}\right]. \quad (43)$$

The Fourier transform $S_{VV}(\omega)$ of the correlation function in the thermodynamical equilibrium state is defined as usual as

$$S_{VV}(\omega) = \int_{-\infty}^{\infty} dt\, e^{i\omega t}\,\langle V(t)\,V(0)\rangle. \quad (44)$$

Under the assumption that most of the spectral weight of the V operator lies in the low-energy region $\hbar\omega \ll k_BT$, we can approximate $1-e^{-\hbar\omega/k_BT} \simeq \hbar\omega/k_BT$. This is a quite standard approximation of many-body theory and is generally accurate in the small q limit [37]. After a few manipulations, it leads to the general expression

$$S_{VV}(t=0) = \int\frac{d\omega}{2\pi}\,S_{VV}(\omega) \simeq \int\frac{d\omega}{2\pi}\,\frac{2k_BT}{\omega}\,\mathrm{Im}[\chi_{VV}(\omega)] = k_BT\,\mathrm{Re}[\chi_{VV}(\omega=0)], \quad (45)$$

where the equivalent of Eq.(26) was used to obtain the last identity. An application of the fluctuation-dissipation relation (45) to the susceptibility and the fluctuations of the mass current in liquid He can be found in [15].

The link between the variance of the deposited energy and the normal fraction is immediately obtained by applying (45) to the specific operator $V = \int d^2r\,\mathbf{j}(\mathbf{r})\,\mathbf{A}(\mathbf{r},0^+)$ and isolating the contribution of the spatially modulated gauge field proportional to $\Omega_p^+\Omega_p^-$. In this way, using Eq.(C10), one is led to the final expression

$$\frac{\pi w^2}{4}\,\frac{\rho}{m}\,\left(\frac{\epsilon_{\rm gauge}}{2}\right)^2 f_n \simeq \simeq \frac{1}{2k_BT}\,\lim_{\gamma\to 0}\langle[H_0(+\infty)-H_0(0)]^2\rangle, \quad (46)$$

which demonstrates an alternative way of extracting the value of the normal fraction f_n from a measurement of the statistical variance of the deposited energy in a series of experiments.

V. OPTICAL MEASUREMENT

The proposal that we have illustrated in the previous section was based on the measurement of atomic quantities, namely the deposited energy in the atomic cloud at the end of the gauge field sequence. The present section is devoted to the presentation and the characterization of an alternative, all-optical route to measure the normal fraction f_n: information on the response of the atomic cloud to the gauge field can be retrieved from the transmitted probe beams once they have crossed the atomic cloud. Recent works have in fact pointed out that the strong frequency-dependence of the dielectric constant of an optically dressed medium in the electromagnetically induced transparency (EIT), already used experimentally to strongly reduce the light group velocity [38–40], can be exploited for velocimetry experiments: Information on the current profile of an atomic cloud was predicted to be imprinted onto the phase of the transmitted probe beam [41, 42]. In the present case, the probe and coupling light consists of the beams respectively oscillating at angular frequencies $\omega_{p,c}$, as sketched in Fig.1. Differently from the case of [41, 42], the current pattern is generated here by the same beams that are then used for probing.

A. Atomic polarization due to non-adiabatic coupling

The transmission and reflection of probe light from the two-dimensional atomic cloud can be described in terms of Maxwell equations. In particular, the dipole polarization of the atoms provides a source term for probe electric

field $\mathcal{E}_p$ at ω_p: for the positive frequency parts, one has in the paraxial approximation with respect to the z axis:

$$(\Delta + k_p^2)\,\mathcal{E}_p = -\frac{k_p^2}{\epsilon_0}\mathcal{P}_p, \tag{47}$$

where $k_p = \omega_p/c$.

Within a perturbative picture, we need to calculate the mean atomic polarization $\mathcal{P}_p$ induced by the unperturbed laser fields. In terms of the three-dimensional atomic field operators, this reads

$$\mathcal{P}_p(\mathbf{r}) = d_{ae}\,\langle \hat{\Psi}_a^\dagger(\mathbf{r})\,\hat{\Psi}_e(\mathbf{r})\rangle. \tag{48}$$

After adiabatic elimination, as shown in the Appendix B, the atomic field in the excited state can be written in terms of the atomic field operator $\hat{\chi}_{3D}$ in the coupled $|C\rangle$ state,

$$\hat{\chi}_{3D}(\mathbf{r},t) = \langle C(\mathbf{r},t)|a\rangle\,\hat{\Psi}_a(\mathbf{r},t) + \langle C(\mathbf{r},t)|b\rangle\,\hat{\Psi}_b(\mathbf{r},t) \tag{49}$$

as

$$\hat{\Psi}_e \simeq \frac{\Omega_c}{2(\delta + i\Gamma/2)}\,[1 + |\Omega_p/\Omega_c|^2]^{1/2}\,\hat{\chi}_{3D} + \Gamma^{1/2}\hat{B}_e. \tag{50}$$

From the explicit form of the noise term $\hat{B}_e$ given in the Appendix B, it is immediate to see that it gives a zero contribution to the mean in Eq.(48). Since the atoms are mostly in the uncoupled $|NC\rangle$ state, we can approximate the atomic field Ψ_a in the $|a\rangle$ state by its $|NC\rangle$ component. To lowest order in Ω_p/Ω_c we then have

$$\mathcal{P}_p(\mathbf{r}) \simeq \frac{d_{ae}\,\Omega_c}{2(\delta + i\Gamma/2)}\,\langle \hat{\phi}_{3D}^\dagger(\mathbf{r})\,\hat{\chi}_{3D}(\mathbf{r})\rangle. \tag{51}$$

The next step is to perturbatively evaluate the field $\hat{\chi}_{3D}$ that is created in the coupled $|C\rangle$ state by the motional coupling [43] of $|C\rangle$ to $|NC\rangle$. The details of the procedure are given in the Appendix B. To first order in Ω_p/Ω_c and for the magic choice Eq.(23) of Δ_c, one obtains after adiabatic elimination

$$\hat{\chi}_{3D} \simeq -\frac{4\hbar(\delta + i\Gamma/2)}{m|\Omega_c|^2}\nabla\,\hat{\phi}_{3D}\cdot\nabla\,\frac{\Omega_p}{\Omega_c} + \Gamma'^{1/2}\hat{B}_\chi. \tag{52}$$

An explicit expression for the noise term $\hat{B}_\chi$ is given in the Appendix B: again, the noise term has a zero expectation value and does not contribute to the optical polarization. The final form of the optical polarization in terms of the atomic density and current operators (17) and (15) reads:

$$\mathcal{P}_p(\mathbf{r}) = -\frac{4\,|d_{ae}|^2}{\hbar\,|\Omega_c|^2}\times$$
$$\times\,(\mathbf{k}_p - \mathbf{k}_c)\cdot\left[\langle \mathbf{j}_{3D}(\mathbf{r})\rangle + \frac{\hbar}{2im}\,\nabla\langle n_{3D}(\mathbf{r})\rangle\right]\,\mathcal{E}_p(\mathbf{r}), \tag{53}$$

where the Rabi frequency of the probe beam has been eliminated in favor of the electric field using the definition $-d_{ea}\mathcal{E}_p = \hbar\Omega_p/2$ and the detuning δ has disappeared from the formula. The first term proportional to the atomic current operator has a simple semi-classical interpretation in terms of the reduced group velocity in the Electromagnetically Induced Transparency regime, as anticipated in [41, 42]: in this regime, the refractive index strongly depends on the Raman detuning, which in turn depends on the atomic speed because of the Doppler effect.

However, the expression (53) differs from the semi-classical one that was used in [42] in two ways. First, the current operator in Eq.(53) differs from the physical current of atoms by the gauge field

$$\mathbf{j}_{\rm phys} = \mathbf{j}_{3D} - \frac{1}{m}\,n_{3D}\,\mathbf{A}_{3D}. \tag{54}$$

As the proposal in [42] addressed a pre-existing current profile and the weak probe beam induced a vanishingly small gauge field, the difference was irrelevant in that case. Here, on the contrary, the mean current is itself proportional to the gauge field so that the difference between the two operators really matters. Second, the expression (53) contains an extra term proportional to the average density gradient. In contrast to the first term, this one is purely imaginary. As a result, it only affects the intensity of the transmitted light via a combination of absorption and/or amplification effects. In particular, as it does not induce any phase shift on the light, it does not interfere with the proposal of [42].

B. Extracting f_n from transmitted light

In order to calculate the modification $\delta\mathcal{E}_p$ induced by the atoms on the transmitted electric field of the probe, one has to insert the polarization (53) as a source term into the Maxwell equation (47). Within a standard approximation, we can neglect diffraction effects stemming from the in-plane part of the Laplace operator in (47) and integrate the z dependence across the atomic cloud. Taking into account the appropriate boundary conditions for $\delta\mathcal{E}_p$, this leads to the expression

$$\delta\mathcal{E}_p(x,y,z) \simeq e^{ik_p z}\,\frac{ik_p}{2\epsilon_0}\int_{-\infty}^{\infty} dz'\,e^{-ik_p z'}\,\mathcal{P}_p(x,y,z') \tag{55}$$

for the transmitted field in the $z > 0$ region. In order for the approximation to be accurate, z has to be much larger than the thickness $a_{\rm ho}^z$ of the atomic pancake, but at the same time much smaller than the diffraction length k_p/q^2, where q is the characteristic wavevector of the in-plane modulation of the atomic density and current.

Along z, the atomic field varies as the harmonic oscillator ground state wavefunction $\phi_0(z)$, see Eq.(19). Performing the integral over z', this gives the final expression for the variation of the transmitted field

$$\delta\mathcal{E}_p(\mathbf{r}) = \frac{2ik_p\,|d_{ae}|^2}{\hbar\epsilon_0\,|\Omega_c|^2}\,\mathbf{k}_c\cdot\left[\langle \mathbf{j}(\mathbf{r})\rangle + \frac{\hbar}{2im}\,\nabla\langle n(\mathbf{r})\rangle\right]\,\mathcal{E}_p(\mathbf{r}) \tag{56}$$

in terms of the two-dimensional density $n(\mathbf{r})$ and current $\mathbf{j}(\mathbf{r})$ operators. The first contribution proportional to the atomic current gives a phase shift, while the second contribution proportional to the atomic density gradient is responsible for absorption and amplification of the probe beam.

The atomic current profile created by the gauge field is evaluated using the linear response formulas (3) and (4) as discussed in detail in the previous sections. The gauge field is assumed to be switched on slowly enough as compared to the characteristic frequencies of all the excitation modes of the gas at wavevector $\mathbf{q}$. Within the linear response regime, the contribution to the current due to the spatially modulated gauge field at $\mathbf{q}$ may be isolated by a suitable combination of measurements with different values of $\Omega_p^{\pm}$, which gives

$$\langle \mathbf{j} \rangle_2(\mathbf{r}) = \frac{\hbar \rho k_c}{mq|\Omega_c|^2} (\mathbf{q} \cos\alpha + f_n \mathbf{e}_z \times \mathbf{q} \sin\alpha) \times \left(\Omega_p^+ \Omega_p^{-*} \, e^{i\mathbf{q}\cdot\mathbf{r}} + \Omega_p^{+*} \Omega_p^- \, e^{-i\mathbf{q}\cdot\mathbf{r}} \right) e^{-2|\mathbf{r}-\mathbf{r}_0|^2/w^2}, \quad (57)$$

where $\mathbf{r}$ is now in the xy plane and α is the oriented angle that $\mathbf{k}_c$ makes with $\mathbf{q}$ [27]. Inserting this expression into (56) and recalling the form (7) of the incident probe field, one can extract the phase shift experienced by the central part of the probe beams after crossing the atomic pancake,

$$\Delta\phi_2^{\pm} = \frac{6\pi\hbar\rho}{m} \frac{|\Omega_p^{\mp}|^2}{|\Omega_c|^4} B\Gamma \, [\cos^2\alpha + f_n \sin^2\alpha], \quad (58)$$

where we have assumed $k_p \simeq k_c$. The total decay rate of the e state by spontaneous emission is indicated by Γ and B is the branching ratio for the decay to the a state, so that $B\Gamma = |d_{ae}|^2 k_c^3/(3\pi\hbar\epsilon_0)$. As we have already mentioned above, the density gradient term in (56) only introduces an intensity modulation and is not responsible for any phase shift.

From a nonlinear optics point of view, the phase shift (58) can be interpreted as arising from a $\chi^{(3)}$ optical nonlinearity of opto-mechanical origin similar to the one that was demonstrated in the experiment [44]: the nonlinear modulation of the optical response of the atoms is determined by the mechanical distortion of the cloud by the optical forces.

Inserting into (58) the values of Table I for the ^{87}Rb case, for the first choice of level scheme reported in the Appendix A, one has a branching ratio $B = 1/4$ and one finds a small, yet appreciable phase shift on the order of

$$\Delta\phi_2^{\text{choice 1}} \simeq 6 \cdot 10^{-4} \times [\cos^2\alpha + f_n \sin^2\alpha]. \quad (59)$$

For the second choice of level scheme in the Appendix A, the branching ratio is slightly larger, $B = 1/3$, but for the compromise choice Eq.(A24) $|\Omega_c|^2/\Gamma^2$ is larger so that one finds a smaller phase shift

$$\Delta\phi_2^{\text{choice 2}} \simeq 3 \cdot 10^{-4} \times [\cos^2\alpha + f_n \sin^2\alpha]. \quad (60)$$

In addition to the phase shift of the transmitted beam that we have discussed so far, Bragg diffraction on the spatially modulated current profile produces a pair of additional beams of in-plane wavevector respectively $\pm 3\mathbf{q}/2$ via a sort of four-wave mixing process. The relative intensity of these beams as compared to the incident probe beams is of the order of $|\Delta\phi_2|^2$. For transverse gauge fields such that $\mathbf{q}\cdot\mathbf{k}_c = 0$ the contribution of the induced density gradient term of (56) vanishes by symmetry. In the case of longitudinal gauge fields, the relative correction is on the order of $q\xi$.

C. Current fluctuations and the angular distribution of scattered light

All the calculations presented in the previous subsections aimed at evaluating the expectation value of the transmitted field amplitude. At this level of the theory, we were allowed to describe the probe beam as a coherent, classical field and we could neglect the fluctuations around the expectation value of both the light field amplitude and the atomic current and density operators. The formalism can be straightforwardly extended to quantum optical fields so to include the fluctuations of the atomic density and current. This is crucial when one aims at investigating the spontaneous scattering of light off the current fluctuations in the atomic gas. In this subsection, we shall in particular show how information on the normal fraction of the gas can be inferred from the angular distribution of scattered light. We shall make the approximation of replacing temporal derivatives of the electromagnetic field $\partial_t \mathcal{E}$ by $-ick_p\mathcal{E}$ in Maxwell's equation. In particular, this misses retardation effects in the expression of the scattered fields in terms of the atomic dipoles, which is accurate since the system size is much smaller than c/Γ.

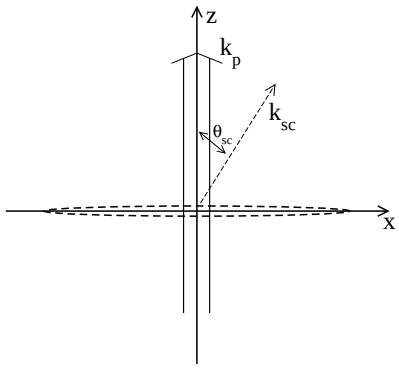

FIG. 5: Scheme of the scattering geometry under examination. Probe light is incident at wavevector $\mathbf{k}_p = k_p\mathbf{e}_z$ and the scattered light is collected at a wavevector $\mathbf{k}_{\text{sc}} = (k_p^2 - Q^2)^{1/2}\,\mathbf{e}_z + \mathbf{Q}$.

We consider the geometry sketched in Fig.5: a single Gaussian probe beam is incident onto the atoms with a wavevector $\mathbf{k}_p$ exactly orthogonal to the atomic plane,

waist w centered at $\mathbf{r}_0$ and a weak peak amplitude $\mathcal{E}_p^0$. Inserting this form into (56) and taking the Fourier transform along the xy plane, one obtains the following operator equation for the scattered field component at in-plane wavevector $\mathbf{Q}$ [47],

$$\mathcal{E}(\mathbf{Q},z) \simeq \frac{2i\,k_p\,|d_{ae}|^2}{\epsilon_0\,\hbar\,|\Omega_c|^2}\,\pi\,w^2\,\mathcal{E}_p^0\int\frac{d^2q}{(2\pi)^2}\,e^{-q^2w^2/4}\,e^{-i\mathbf{q}\cdot\mathbf{r}_0} \times\left\{\mathbf{k}_c\cdot\left[\mathbf{j}_{\mathbf{Q}-\mathbf{q}}+\frac{\hbar(\mathbf{Q}-\mathbf{q})}{2m}\,n_{\mathbf{Q}-\mathbf{q}}\right]\right\}e^{ik_z(\mathbf{Q})\,z}. \quad (61)$$

Here, $\mathbf{j}_\mathbf{Q}$ and $n_\mathbf{Q}$ are the spatial Fourier transforms of the two-dimensional current $\mathbf{j}(\mathbf{r})$ and density $n(\mathbf{r})$ operators; the Fourier transform of a product of two functions has been rewritten in terms of the convolution of their Fourier transforms. The z component of the propagation wavevector is determined by the photon dispersion as $k_z=(k_p^2-Q^2)^{1/2}$.

The intensity of the scattered light at in plane wavevector $\mathbf{Q}$ is quantified by [47]

$$\langle\mathcal{E}^\dagger(\mathbf{Q})\mathcal{E}(\mathbf{Q})\rangle=\left[\frac{2\pi k_p\,|d_{ae}|^2\,w^2\,|\mathcal{E}_p^0|}{\epsilon_0\,\hbar\,|\Omega_c|^2}\right]^2\times \int\frac{d^2q}{(2\pi)^2}\int\frac{d^2q'}{(2\pi)^2}\left\langle\left\{\mathbf{k}_c\cdot\left[\mathbf{j}^\dagger_{\mathbf{Q}-\mathbf{q}}+\frac{\hbar(\mathbf{Q}-\mathbf{q})}{2m}\,n^\dagger_{\mathbf{Q}-\mathbf{q}}\right]\right\} \times\left\{\mathbf{k}_c\cdot\left[\mathbf{j}_{\mathbf{Q}-\mathbf{q}'}+\frac{\hbar(\mathbf{Q}-\mathbf{q}')}{2m}\,n_{\mathbf{Q}-\mathbf{q}'}\right]\right\}\right\rangle \times e^{i(\mathbf{q}-\mathbf{q}')\cdot\mathbf{r}_0}e^{-(q^2+q'^2)\,w^2/4} \quad (62)$$

Since the system size is much larger than the waist w of the probe beam, we can for simplicity assume an effective translational symmetry along the xy plane. As a consequence, the correlation function that appears in (62) has a delta-function shape around equal wavevectors $\mathbf{Q}-\mathbf{q}=\mathbf{Q}-\mathbf{q}'$ (see e.g. the next Eq.(63)).

In contrast to the schemes proposed in the previous sections, where the duration $1/\gamma$ of the experiment had to be at least on the order of $1/(c_sq)$, the light scattering experiment discussed here can be performed on a much faster time scale, only limited by the characteristic rate Γ' of the internal atomic evolution time, Eq.(B7). As a result, the experiment can be performed in the small wavevector region $Q\xi\ll1$ where the contribution to (62) of the terms involving the density fluctuations $n_\mathbf{Q}$ is negligible [63]. Of course, efficient isolation of the scattered light from the incident beam requires that the scattering angle $\theta_{\rm sc}\simeq Q/k_p$ be much larger than the diffraction cone of the probe beam, i.e. $Q\gg1/w$.

The instantaneous correlation function of the current in the y direction parallel to $\mathbf{k}_c$ can be evaluated applying the fluctuation-dissipation relation (45) to the current operator $\mathbf{j}_\mathbf{q}$ in an infinite space geometry. This gives

$$\langle j^\dagger_{\mathbf{Q},y}\,j_{\mathbf{Q}',y}\rangle=(2\pi)^2\,\delta^2(\mathbf{Q}-\mathbf{Q}')k_BT\,{\rm Re}[\chi_{yy}(\mathbf{Q}',\omega=0)] \underset{Q\to0}{\simeq}(2\pi)^2\,\delta^2(\mathbf{Q}-\mathbf{Q}')\frac{k_BT\,\rho(\mathbf{r}_0)}{m} \times[\cos^2\phi_{\rm sc}+f_n\sin^2\phi_{\rm sc}], \quad (63)$$

where $\phi_{\rm sc}$ is now the azimuthal angle between $\mathbf{k}_c$ and $\mathbf{Q}$. Inserting this expression into (62) and taking the thermodynamic limit, one gets to the final expression for the scattered intensity in the momentum $\mathbf{Q}$-space [47],

$$\langle\mathcal{E}^\dagger_\mathbf{Q}\mathcal{E}_\mathbf{Q}\rangle=\left[\frac{k_p\,k_c\,|d_{ae}|^2}{\epsilon_0\,\hbar\,|\Omega_c|^2}\right]^2\,2\pi w^2\,|\mathcal{E}_p^0|^2 \times\frac{k_BT\,\rho(\mathbf{r}_0)}{m}\,[\cos^2\phi_{\rm sc}+f_n\sin^2\phi_{\rm sc}]. \quad (64)$$

To estimate the relative intensity of scattered light, it is useful to rewrite the expression (64) for the momentum space intensity $\langle\mathcal{E}^\dagger_\mathbf{Q}\mathcal{E}_\mathbf{Q}\rangle$ in terms of physically more transparent quantities such as the angular distribution $I(\theta_{\rm sc},\phi_{\rm sc})$ of scattered intensity. For small scattering angles $|\theta_{\rm sc}|\ll1$, the infinitesimal solid angle and momentum space volume elements are related by $d\Omega=\sin\theta_{\rm sc}\,d\theta_{\rm sc}\,d\phi_{\rm sc}\simeq\theta_{\rm sc}\,d\theta_{\rm sc}\,d\phi_{\rm sc}\simeq d^2Q/k_p^2$, so that

$$I_{\rm sc}(\theta_{\rm sc},\phi_{\rm sc})\simeq\frac{k_p^2}{(2\pi)^2}\,\langle\mathcal{E}^\dagger_\mathbf{Q}\mathcal{E}_\mathbf{Q}\rangle. \quad (65)$$

This immediately leads to the final expression for the angular distribution of the scattering intensity [47]

$$\frac{I_{\rm sc}(\theta_{\rm sc},\phi_{\rm sc})}{I_{\rm inc}}=\left[\frac{k_p^2\,k_c\,|d_{ae}|^2}{\pi\epsilon_0\,\hbar\,|\Omega_c|^2}\right]^2\frac{k_BT\rho(\mathbf{r}_0)}{m}\times [\cos^2\phi_{\rm sc}+f_n\sin^2\phi_{\rm sc}] \quad (66)$$

in units of the incident intensity,

$$I_{\rm inc}=\int d^2r\,|\mathcal{E}_p(\mathbf{r})|^2=\frac{\pi w^2}{2}\,|\mathcal{E}_p^0|^2 \quad (67)$$

From this expression, it is immediate to see that information on the normal fraction of the gas can be retrieved from the azimuthal dependence of the scattered intensity. In terms of the spontaneous emission decay rate Γ of the e state and the branching ratio B, Eq.(66) can be rewritten in the more transparent form [47],

$$\frac{I_{\rm sc}}{I_{\rm inc}}\;=\;\frac{9}{2\pi}\frac{k_B^2TT_d}{\hbar^2}\frac{B^2\Gamma^2}{|\Omega_c|^4}[\cos^2\phi_{\rm sc}\,+\,f_n\sin^2\phi_{\rm sc}]. \quad (68)$$

To estimate the feasibility of the proposed light scattering experiment, we now derive an upper bound on the number of useful scatterered photons in a single shot of duration τ. Calculating the Poynting's vector of the probe beam, and using (67), we find an incident flux of

probe photons $\Phi_{\rm inc} = (k_p w)^2 |\Omega_p^0|^2/(12B\Gamma)$. Integrating in (66) the term proportional to f_n over solid angles in the cone $\theta_{\rm sc} \leq 1/(k_p\xi)$, we obtain the flux $\Phi_{\rm sc}^{\rm use}$ of useful scattered photons. As a maximal duration, we take $\tau = 1/\Gamma_{\rm fluo}^{\rm non-ad}$ where the fluorescence rate of the atoms due to motional coupling between the non-coupled and the coupled states is given by Eq.(A2) (with $2|\Omega_p^+|^2$ replaced here with $|\Omega_p^0|^2$). The number of single shot useful scattered photons is thus bounded by

$$N_{\rm ph}^{\rm use} \leq \frac{3\pi B}{16}\frac{k_B T}{\hbar\omega_z}\rho w^2 f_n \frac{1}{(k_c\xi)^2}. \qquad (69)$$

Remarkably the Rabi frequencies Ω_c and Ω_p^0 have cancelled out in the ratio of the scattered flux to the fluorescence rate. One recognizes in the right-hand side of (69) the effective mean number of atoms $N_{\rm at}^{\rm eff} = \pi\rho w^2 f_n/4$ in the normal component illuminated by the probe beam, as in Eq.(27). There is however a severe geometrical reduction factor, $1/(k_c\xi)^2$, due to the small aperture of the useful scattering cone. For the parameters of Table I, with $B = 1/3$, and taking a waist $w = 30\xi$ and $f_n = 0.2$ as in Fig.4, we find $N_{\rm at}^{\rm eff} \simeq 1400$, $1/(k_c\xi) \simeq 0.15$, which leads to $N_{\rm ph}^{\rm use} \leq 5$. This remains accessible to current quantum optics experiments. For $k_B T/\hbar\omega_z$ fixed, the upper bound in Eq.(69) scales as ρ^2, since $1/\xi^2$ scales as ρ, so that larger values of photon numbers for a given waist may be obtained by increasing the density ρ of the bidimensional Bose gas.

VI. CONCLUSIONS AND PERSPECTIVES

In this paper we have proposed and validated two methods to measure the superfluid fraction of a quantum fluid of ultracold atoms. The idea is to apply an artificial gauge field to the atoms with spatial oscillations within a localized envelope and to detect, within the linear response regime, the current pattern that is generated in the fluid. This can be done either in a mechanical way by measuring the energy that is deposited in the fluid at the end of a gauge field sequence, or in an all-optical way by observing the phase shift experienced by the same laser beams that are used to generate the artificial gauge field or the angular pattern of scattered light.

The interest of the proposed methods is twofold: they do not require that the gas reaches thermal equilibrium in presence of the gauge field, and furthermore they give the possibility of reconstructing in a local way the spatial profile of the superfluid fraction of a trapped gas, independently from the presence or the absence of a Bose-Einstein condensate. This last feature is attractive in the study of the Berezinskii-Kosterlitz-Thouless transition to a superfluid state in two-dimensional Bose gases and of the superfluidity properties of Bose gases in disordered environments. It would also be interesting to extend the method to the study of superfluidity in multi-component atomic fermionic gases, which may require identification of suitable level schemes.

Acknowledgments

We acknowledge useful discussions with G. La Rocca, S. Stringari, F. Gerbier, C. Salomon and J. Dalibard. The work of Y.C. was done as part of the ERC FERMIX project. I.C. acknowledges financial support from ERC through the QGBE grant.

Appendix A: Experimental issues

2D density	$\rho\lambda_c^2 = 9$	$\rho = 14\mu\text{m}^{-2}$
degeneracy temperature	$k_B T_d \equiv 2\pi\hbar^2\rho/m$	$T_d = 500$ nK
temperature	$T = 0.1\,T_d$	$T = 50$ nK
2D interaction constant	$\tilde{g} = mg/\hbar^2$	$\tilde{g} = 0.1$
transverse confinement	$\hbar\omega_z = 0.23\,\hbar^2 k_c^2/m$ $= 0.16\,k_B T_d$	$\frac{\omega_z}{2\pi} = 1.65$ kHz
healing length	$\xi \equiv (\rho\tilde{g})^{-1/2}$	$\xi = 0.84\mu m$

reduced gauge field amplitude	$\tilde{\epsilon}_{\rm gauge} \equiv \frac{\epsilon_{\rm gauge}}{(mk_B T_d)^{1/2}}$	$\tilde{\epsilon}_{\rm gauge} = 0.15$
probe beam Rabi frequencies	$\frac{(\lvert\Omega_p^+\rvert^2 + \lvert\Omega_p^-\rvert^2)_{t=0+}}{2\lvert\Omega_c\rvert^2}$	0.09
gauge field switch-off rate	$\gamma = 0.2\,c_s q$ with $q = 1/\xi$	$1/\gamma = 4.8$ ms $q = 0.15 k_c$

	first choice	second choice
coupling Rabi frequency $\lvert\Omega_c\rvert^2/\Gamma^2$	0.21	0.5
minimum detuning δ/Γ	1	1.5
fluorescence probability $P_{\rm fluo}$	0.22	0.045
spurious deposited energy $\Delta E_U/\Delta E_2$ (for $f_n = 0.2$)	33	0.16

TABLE I: Suggested values of the physical parameters for an experimental measurement of the normal fraction of a two-dimensional Bose gas of ^{87}Rb using an artificial gauge field produced by laser (coupling and probe beam) excitation on the D1 line at $\lambda_c = 795$ nm. The first block characterizes the thermal equilibrium of the gas. The second block determines the gauge field. The third block deals with the issues related to the spontaneous emission and the spurious lightshift. The three-dimensional scattering length is estimated to be $a_{3D} =$ 100 Bohr radii and is related to the two-dimensional coupling constant by Eq.(20). A useful relation is $m\Gamma/(\hbar k_c^2) \simeq 792$.

In this Appendix we review some issues that may hinder an experimental implementation of our proposal. Our attention will be concentrated onto the most relevant case of ^{87}Rb atoms considered in the experiment of [45, 46]

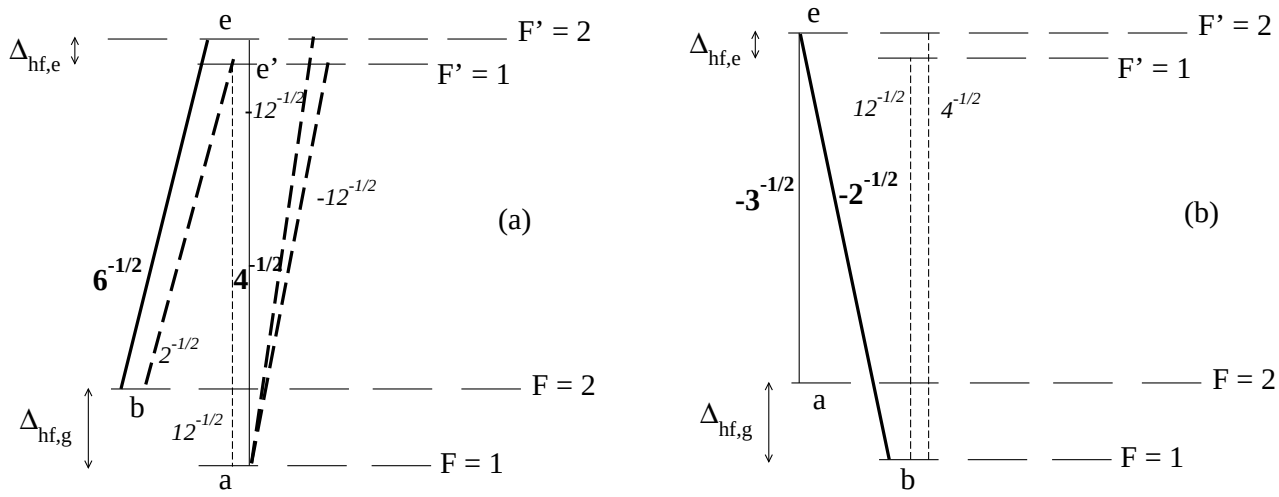

FIG. 6: Scheme of the internal levels of ^{87}Rb atom involved in the D_1 transition ($J = 1/2 \to J' = 1/2$). The hyperfine splitting of the ground (excited) state is $\Delta_{\rm hf,g} = 2\pi \times 6.834\,{\rm GHz}$ ($\Delta_{\rm hf,e} = 2\pi \times 814\,{\rm MHz}$). The natural linewidth of the excited state is $\Gamma = 2\pi \times 5.75\,{\rm MHz}$. Narrow (thick) lines indicate transitions that are induced by the coupling (probe) beams. Solid (dashed) lines indicate the desired (main undesired) transitions. The relevant dipole matrix elements are shown in units of the reduced dipole element $\langle J = 1/2||er||J' = 1/2\rangle$ of the D1 line, in boldface for the desired transitions and in italic for the undesired ones. Our first choice for the Λ system $|a\rangle, |e\rangle, |b\rangle$ states is shown in the left (a) panel, with $|a\rangle = |F = 1, m_F = -1\rangle$, $|e\rangle = |F' = 2, m_{F'} = -1\rangle$, $|b\rangle = |F = 2, m_F = -2\rangle$. The second choice is shown in the right (b) panel, with $|a\rangle = |F = 2, m_F = -2\rangle$, $|e\rangle = |F' = 2, m_{F'} = -2\rangle$, $|b\rangle = |F = 1, m_F = -1\rangle$. Note that we have taken the y axis as the quantization axis of angular momenta.

and, in a two-dimensional context, in [4]. The level structure of this atomic species is sketched in Fig.6. A possibly important advantage of this atom in view of an experimental implementation of the present proposal is that the singlet and triplet scattering lengths of ground state atoms are equal within a few percent [49]. We thus expect that all scattering lengths between arbitrary $F = 1$ or $F = 2$ sublevels of the ground state have all almost the same values [50], which leads to $g_{aa} \simeq g_{ab}$ and therefore to a suppression of the spatio-temporal variation of the effective interaction constant $g_{3D}(\mathbf{r}, t)$ defined in (18). In the deposited energy method proposed in Sec.IV, this is important to reduce emission of phonons in the atomic gas by the temporal modulation of the interaction constant. In the optical detection scheme of Sec.V, this is also important to suppress the contribution of the interaction term to the field $\hat{\chi}_{3D}$ and then to the optical polarization. Other atomic species such as Yb [17] or metastable He [18, 19] and/or different laser beam configurations [20, 21] are expected to be useful for other purposes, e.g. to suppress spontaneous emission and/or generate artificial gauge fields with different geometries [64]

Two possible choices for the three states $|a\rangle, |b\rangle, |e\rangle$ forming the Λ system on the $D1$ line of ^{87}Rb are considered, as sketched in the two panels of Fig.6. For each choice, we determine the undesired effects (spontaneous emission, lightshifts, Raman leaks) stemming from deviations from the perfect adiabatic following of the non-coupled state by the moving atoms and from optical transitions to other levels not included in the Λ system. An eye will also be kept on trying to maximize the e to a branching ratio so as to reinforce the optical signal of Sec.V. To minimize spontaneous emission within the low saturation regime, we shall allow for a small detuning δ of both the probe and coupling beam carrier frequencies from the $|a\rangle \to |e\rangle$ and $|b\rangle \to |e\rangle$ transitions, respectively. The detuning of the two beams is taken in a way to always fulfill the magic Raman condition (23).

a. *First choice*

The coupling beam propagates along the y axis and is taken with a σ_+ polarization (along y axis). The probe beam is taken as linearly polarized along y. For the three atomic levels forming the Λ system, we take $|a\rangle \equiv |F = 1, m_F = -1\rangle$, $|b\rangle \equiv |F = 2, m_F = -2\rangle$ and $|e\rangle \equiv |F' = 2, m_{F'} = -1\rangle$ [65]. This scheme of levels and lasers is illustrated in the left panel (a) of Fig.6.

To estimate the importance of the non-adiabatic coupling between the $|NC\rangle$ and the $|C\rangle$ states due to the atomic motion, we can evaluate the ratio ρ_C/ρ_{NC} of the two-dimensional densities in the two states close to the center of the laser spot. This is done using the explicit formula (52) for the field in the $|C\rangle$ state [66]. Using the fact that for quasi-2D samples the gradient is mostly along the harmonically trapped z direction and assuming $\Omega_p^+ = \Omega_p^-$, we obtain for $k_p \simeq k_c$:

$$\frac{\rho_C}{\rho_{NC}} \simeq \left| \frac{4(\delta + i\Gamma/2) k_c\, \Omega_p^+}{\Omega_c^3} \right|^2 \frac{\hbar\omega_z}{m}. \qquad \text{(A1)}$$

Accuracy of the adiabatic approximation requires that this ratio is much smaller than unity.

The finite population that is present in the $|C\rangle$ state as a consequence of non-perfect adiabaticity is responsible for the spontaneous emission of photons at a single atom rate:

$$\Gamma_{\rm fluo}^{\rm non-ad} = \Gamma' \frac{\rho_{NC}}{\rho_C} = 4\Gamma \frac{|\Omega_p^+|^2}{|\Omega_c|^4} \frac{\hbar k_c^2}{m} \omega_z, \qquad \text{(A2)}$$

where the fluorescence rate Γ' of the coupled state $|C\rangle$ is defined by Eq.(11) and a spatial average has been performed. Remarkably, $\Gamma_{\rm fluo}^{\rm non-ad}$ does not depend on the detuning δ.

Other contributions to the fluorescence rate come from non-resonant excitation processes. Dominating among these are the excitation of the $|a\rangle$ state to the states $|F' = 1 \text{ or } 2, m_{F'} = 0\rangle$ by the coupling beam at a rate

$$\Gamma_{\rm fluo}^{c} = \Gamma \frac{|\Omega_c|^2}{4\Delta_{\rm hf,g}^2}, \qquad \text{(A3)}$$

and the excitation of the non-coupled state $|NC\rangle$ to $|e'\rangle = |F' = 1, m_{F'} = -1\rangle$ by the total probe plus coupling field with an effective Rabi frequency $-2\Omega_p/\sqrt{3}$, which results in the fluorescence rate on the parasitic Λ' configuration $|a\rangle \to |e'\rangle \to |b\rangle$:

$$\Gamma_{\rm fluo}^{\Lambda'} = \frac{2}{3}\Gamma \frac{|\Omega_p^+|^2}{\Delta_{\rm hf,e}^2}. \qquad \text{(A4)}$$

In these expressions, we have taken into account the tabulated hyperfine dipole matrix elements of the various optical transitions, and we have introduced the hyperfine splittings $\Delta_{\rm hf,g}$ and $\Delta_{\rm hf,e}$ given for ^{87}Rb in the caption of Fig.6. Limiting ourselves to the most relevant regime where $|\Omega_p^+/\Omega_c|^2 > 1/100$, we see that in the present case of ^{87}Rb atoms, $\Gamma_{\rm fluo}^{\Lambda'} \gg \Gamma_{\rm fluo}^{c}$.

The total fluorescence rate can then be approximated as the sum of $\Gamma_{\rm fluo}^{\Lambda'}$ and $\Gamma_{\rm fluo}^{\rm non-ad}$. For a given value of the gauge field (proportional to $|\Omega_p^+/\Omega_c|^2$), the total fluorescence rate is minimized to

$$\Gamma_{\rm fluo}^{\rm min} \simeq \frac{4\sqrt{6}}{3} \left|\frac{\Omega_p^+}{\Omega_c}\right|^2 \frac{\Gamma}{\Delta_{\rm hf,e}} \left(\frac{\hbar k_c^2 \omega_z}{m}\right)^{1/2} \qquad \text{(A5)}$$

by a careful choice of the coupling beam Rabi frequency

$$\left|\Omega_c^{\rm opt}\right|^2 = \Delta_{\rm hf,e} \sqrt{\frac{6\hbar k_c^2\, \omega_z}{m}} = \frac{\sqrt{3}\Delta_{\rm hf,e}}{2\pi^{1/2}} \frac{\hbar k_c}{m a_{3D}} \tilde{g}. \qquad \text{(A6)}$$

Here, we have expressed ω_z in terms of the three-dimensional scattering length a_{3D} and the reduced two-dimensional coupling constant as given by Table I and Eq.(20). Inserting the actual parameters of the ^{87}Rb atom, and taking $\tilde{g} = 0.1$, we obtain $|\Omega_c^{\rm opt}|^2/\Gamma^2 \simeq 0.21$. It remains to adjust the detuning δ to be in the weak saturation regime,

$$s \equiv \frac{|\Omega_c|^2/2}{|\delta + i\Gamma/2|^2} \lesssim \frac{1}{10}. \qquad \text{(A7)}$$

Let us take the same values of the gauge field sequence as in Fig.4: $\gamma/c_s q = 0.2$ and $q\xi = 1$ and $\epsilon_{\rm gauge} \simeq 0.15(m k_B T_{\rm d})^{1/2}$. This choice of $\epsilon_{\rm gauge}$ leads to $|\Omega_p^+(0^+)/\Omega_c|^2 \simeq 0.03(\rho\lambda_c^2)^{1/2}$: as this quantity has to be much smaller than 1 in order for the gauge field description of Sec.III to be valid, it is safe to impose $\rho\lambda_c^2 < 10$. Integrating over the exponential switch-off ramp of Ω_p and eliminating g in terms of ω_z and a_{3D}, this gives for the total fluorescence probability per atom,

$$P_{\rm fluo} = \frac{\sqrt{6}}{2} \frac{\Gamma}{\Delta_{\rm hf,e}} \left(\frac{k_B T_d \hbar \omega_z}{\rho^2 g^2}\right)^{1/2} = \frac{\sqrt{6}}{4} \frac{\Gamma}{\Delta_{\rm hf,e}} \frac{1}{(\rho a_{3D}^2)^{1/2}}. \qquad \text{(A8)}$$

For ^{87}Rb with the choice $\rho\lambda_c^2 = 9$, we obtain the not very impressive result,

$$P_{\rm fluo} \simeq 0.20\,. \qquad \text{(A9)}$$

For the sake of completeness, it is important to note that for this choice, $k_B T = 0.1 k_B T_d$ remains smaller than $\hbar\omega_z$, so that the Bose gas retains a two-dimensional character.

The existence of other atomic levels in addition to the ones strictly needed to create the gauge field is responsible not only for dissipative effects such as fluorescence, but also creates reactive effects such as a spatially and temporally-dependent light shift of the non-coupled state $|NC\rangle$. Among the dominating processes, the parasitic Λ' scheme creates a modulated light-shift potential

$$U^{\Lambda'}(\mathbf{r}) = \frac{\hbar\,|\Omega_p(\mathbf{r})|^2}{3\Delta_{\rm hf,e}}. \qquad \text{(A10)}$$

A shift of the same order of magnitude arises from the coupling of the a state to the $|F' = 2 \text{ or } 1, m_{F'} = 0\rangle$ by the coupling beam.

An estimate of the energy deposited in the system by the $U^{\Lambda'}$ term as compared to the one ΔE_2 due to the gauge field can be obtained with Bogoliubov theory: Using Eq.(D15) with $\mathcal{U}_0 = \hbar(\Omega_p^+\Omega_p^{-*})(0^+)/(3\Delta_{\rm hf,e})$, $\eta = \gamma$ and $\mathbf{Q} = \mathbf{q}$, one gets for $\hbar\gamma \ll \epsilon_q \ll \rho g$:

$$\frac{\Delta E_{U^{\Lambda'}}}{\Delta E_2} = \frac{|\Omega_c|^4}{9 f_n (k_c c_s)^2 \Delta_{\rm hf,e}^2}. \qquad \text{(A11)}$$

For actual parameters, the energy change due to $\Delta U^{\Lambda'}$ turns out to be non negligible. For the optimal value of the Rabi frequency $\Omega_c^{\rm opt}$ from Eq.(A6), the ratio is

$$\frac{\Delta E_{U^{\Lambda'}}}{\Delta E_2} = \frac{2\hbar\omega_z}{3 f_n\, \rho g}. \qquad \text{(A12)}$$

For ^{87}Rb, one finds the discouraging result $\Delta E_{U^{\Lambda'}}/\Delta E_2 \simeq 600\tilde{g}/(\rho\lambda_c^2 f_n)$, which remains much larger than unity even for $\rho\lambda_c^2 = 9$.

Even if the deposited energy by the spurious potential $U^{\Lambda'}$ is much larger than the desired one of the gauge field, a suitable extrapolation procedure may take advantage of the different dependence on the laser intensities to isolate the effect of the gauge potential. An alternative possibility is to exploit the fact that the $\Delta E_U^{\Lambda'}$ contribution does

not depend on the direction of $\mathbf{q}$: Within the regime of linear response, this contribution can therefore be eliminated by taking the difference of the energy changes for respectively longitudinal and transverse gauge fields.

Another possible nuisance is the existence of stimulated Raman processes that may out couple the non-coupled $|NC\rangle$ state to atomic ground state sublevels $|c\rangle$ other than $|a\rangle$ and $|b\rangle$, via excited state sublevels other than $|e\rangle$ [67]. One may however check that for the proposed scheme these leaky Raman coupling are detuned from resonance by a frequency amount at least $\Delta_{\rm hf,g}$ in absolute value and therefore harmless.

b. *Second choice*

Another possible choice for ^{87}Rb atoms is to take a σ_- polarization for the coupling beam propagating along the y axis. The probe beam is again linearly polarized along y. The atomic levels forming the Λ system are now $|a\rangle \equiv |F=2, m_F=-2\rangle$, $|b\rangle \equiv |F=1, m_F=-1\rangle$ and $|e\rangle \equiv |F'=2, m_{F'}=-2\rangle$. The strong two-body losses that are generally experienced by the upper hyperfine manifold of the ground state are here suppressed by the choice of a maximal m_F state for $|a\rangle$: as collisions between ultra-cold atoms mostly occur in the s-wave scattering channel, conservation of the sum of the m_F's then prevents transition to the lower hyperfine manifold.

The fluorescence rate per atom due to the motional coupling between $|NC\rangle$ and $|C\rangle$ is still given by $\Gamma_{\rm fluo}^{\rm non-ad}$ as defined in Eq.(A2). As there is no longer any parasitic Λ' system, the fluorescence due to laser excitation of $|a\rangle$ or $|b\rangle$ to excited state sublevels other than $|e\rangle$ is now dominated by the transitions $|b\rangle \to |F'=1 \text{ or } 2, m_{F'}=-1\rangle$ due to the probe beam. Thanks to the reduced occupation probability $\simeq |\Omega_p|^2/|\Omega_c|^2$ of sublevel $|b\rangle$ in the atomic state $|NC\rangle$ and to the larger hyperfine splitting $\Delta_{\rm hf,g}$ of the ground state, the fluorescence rate is strongly suppressed. After spatial averaging it amounts to

$$\Gamma_{\rm fluo}^{p} = \frac{3}{2}\Gamma \frac{|\Omega_p^+|^4}{\Delta_{\rm hf,g}^2 |\Omega_c|^2}. \tag{A13}$$

Other fluorescence processes on the D2 line (e.g. the transition $|a\rangle \to |J'=3/2, F'=3, m_{F'}=-3\rangle$ excited by the coupling beam) are several orders of magnitude weaker than $\Gamma_{\rm fluo}^{p}$ thanks to the huge fine structure splitting of $(2\pi)\,7$ THz.

Since the two terms in the sum $\Gamma_{\rm fluo}^{\rm non-ad} + \Gamma_{\rm fluo}^{p}$ experience different switch-off functions $e^{-\gamma t}$ and $e^{-2\gamma t}$, we first integrate over time to calculate the total fluorescence probability, and then optimize over the coupling beam intensity. The minimal fluorescence probability

$$P_{\rm fluo}^{\rm min} = \frac{2\sqrt{3}}{\gamma}\frac{\Gamma}{\Delta_{\rm hf,g}}\left|\frac{\Omega_p^+(0^+)}{\Omega_c}\right|^3 \left(\frac{\hbar k_c^2}{m}\omega_z\right)^{1/2} \tag{A14}$$

is obtained for a coupling beam Rabi frequency such that

$$|\Omega_c^{\rm opt}|^4 = \frac{16}{3}\frac{|\Omega_c|^2}{|\Omega_p^+|^2}\Delta_{\rm hf,g}^2 \frac{\hbar k_c^2}{m}\omega_z. \tag{A15}$$

Introducing the reduced quantities $\tilde\gamma = \hbar\gamma/(\rho g)$ and $\tilde\epsilon_{\rm gauge} = \epsilon_{\rm gauge}/(m k_B T_d)^{1/2}$, and eliminating ω_z in terms of g and a_{3D}, we finally obtain

$$P_{\rm fluo}^{\rm min} = \left(\frac{9}{128\pi}\right)^{1/4} \frac{\tilde\epsilon_{\rm gauge}^{3/2}}{\tilde\gamma}\frac{\Gamma}{\Delta_{\rm hf,g}}\frac{\lambda_c}{a_{3D}}(\rho\lambda_c^2)^{-1/4}. \tag{A16}$$

For the parameters of Table I, in particular $\rho\lambda_c^2 = 9$, one finds $|\Omega_c^{\rm opt}|^2/\Gamma^2 \simeq 5.5$ so that a detuning $|\delta| > 5\Gamma$ is required to remain in the weak saturation regime. This resulting probability of spontaneous emission per atom in the deposited energy measurement is very small,

$$P_{\rm fluo} \simeq 0.008. \tag{A17}$$

As compared to the first one, this second choice then provides a strong reduction of the spontaneous emission rate by a factor almost 30.

Another advantage of this second choice is that there are no longer resonant leaky Raman processes and that lightshift effects are potentially smaller thanks to the absence of the parasitic Λ' scheme. The probe beam on the $|b\rangle \to |F'=1 \text{ or } 2, m_{F'}=-1\rangle$ transitions produces a lightshift which, after average in the $|NC\rangle$ state, leads to the spurious potential

$$U^p(\mathbf{r}) = -\frac{\hbar|\Omega_p|^4}{4|\Omega_c|^2\Delta_{\rm hf,g}}. \tag{A18}$$

The amount of energy that is deposited in the gas by this spurious potential can be estimated using twice Eq.(D15), first with $\mathcal{U}_0 = -\hbar|\Omega_p^+(t=0^+)|^4/(|\Omega_c|^2\Delta_{\rm hf,g})$, $\eta = 2\gamma$, $\mathbf{Q} = \mathbf{q}$, and second with $\mathcal{U}_0$ four times smaller, $\eta = 2\gamma$, $\mathbf{Q} = 2\mathbf{q}$. Neglecting $2\hbar\gamma$ with respect to ϵ_q, and taking $q\xi = 1$, we obtain the following estimate for the spurious deposited energy

$$\Delta E_{U^p} = \frac{133}{160}\frac{N}{\rho g}\frac{\hbar^2|\Omega_p^+(0^+)|^8}{|\Omega_c|^4\Delta_{\rm hf,g}^2}. \tag{A19}$$

For the coupling beam Rabi frequency (A15) minimizing spontaneous emission, the ratio of the energies deposited by the gauge field and the spurious potential amounts to:

$$\frac{\Delta E_{U^p}}{\Delta E_2} = \frac{133\sqrt{2}}{960\pi^{3/2}}\frac{\tilde g\,\tilde\epsilon_{\rm gauge}}{f_n}\frac{\lambda_c}{\rho^{1/2}a_{3D}^2}. \tag{A20}$$

For $\tilde g = 0.1$ and $\tilde\epsilon_{\rm gauge} = 0.15$ and using the ^{87}Rb parameters summarized in Table I, one finds the still quite unfortunate result

$$\frac{\Delta E_{U^p}}{\Delta E_2} \simeq \frac{4}{f_n} \gg 1. \tag{A21}$$

A possibility to overcome this difficulty and separate ΔE_2 from ΔU^p is to use the same strategy proposed to separate ΔE_2 from ΔE_1 by exploiting the different dependence of the two quantities on the ratio $|\Omega_p^+/\Omega_p^-|(0^+)$. Another option is to look for a compromise value of $|\Omega_c|^2/\Gamma^2$ that allows to effectively suppress the lightshift potential without introducing a too large spontaneous emission rate.

To this purpose, we fix $\tilde{\epsilon}_{\rm gauge} = 0.15$, $\gamma = 0.2\rho g/\hbar$, $q\xi = 1$, $\tilde{g} = 0.1$ and we take as free parameters $X = \rho\lambda_c^2$ and $Y = |\Omega_c|^2/\Gamma^2$. Inserting the relevant parameters for ^{87}Rb as in Table I, we obtain

$$P_{\rm fluo} = \frac{6.86\cdot 10^{-2}}{X^{1/2}Y} + 7.46\cdot 10^{-4}Y, \qquad \text{(A22)}$$

$$\frac{\Delta E_{U^p}}{\Delta E_2} = \frac{0.132Y^2}{f_n}. \qquad \text{(A23)}$$

A reasonable compromise between the two competing effects is to choose $X = 9$ and $Y = 0.5$, which corresponds to

$$\rho\lambda_c^2 = 9 \quad \text{and} \quad \frac{|\Omega_c|^2}{\Gamma^2} = 0.5 \quad . \qquad \text{(A24)}$$

As a result, for the same parameters $T/T_d = 0.1$ and $f_n = 0.2$ used in the classical field simulations of section IV, we obtain the quite encouraging values

$$P_{\rm fluo} \simeq 0.045 \qquad \text{(A25)}$$

$$\frac{\Delta E_{U^p}}{\Delta E_2} \simeq 0.16 \quad . \qquad \text{(A26)}$$

To conclude, we have checked that at the resulting temperature $k_BT/\hbar\omega_z = 0.62$ the Bose gas retains a two-dimensional and that the validity of the gauge field model of Sec.III is guaranteed by the resulting probe beam Rabi frequency $|\Omega_p^+(0^+)|^2/|\Omega_c|^2 = 0.03X^{1/2} = 0.09 \ll 1$.

Appendix B: Dum-Olshanii theory for many-body systems

In a seminal work [16], Dum and Olshanii have shown that an effective gauge field appears in the theoretical description of a three-level atom interacting with a laser field on a Λ transition. Here we use the formalism of the Quantum Stochastic Differential Equations (see e.g.§8.3.2 of [25]) to extend this idea to an interacting Bose gas in second quantized form.

We start with the master equation for the density operator $\hat{\sigma}$ of the many-body system, assuming for simplicity that spontaneous emission corresponds to a net loss of atoms,

$$\frac{d}{dt}\hat{\sigma} = \frac{1}{i\hbar}[H,\hat{\sigma}] + \Gamma\int d^3r\,\left[\hat{\Psi}_e(\mathbf{r})\hat{\sigma}\hat{\Psi}_e^\dagger(\mathbf{r}) - \frac{1}{2}\{\hat{\Psi}_e^\dagger(\mathbf{r})\hat{\Psi}_e(\mathbf{r}),\hat{\sigma}\}\right]. \qquad \text{(B1)}$$

The Hamiltonian H is the sum of the single-particle kinetic and trapping terms, of the interaction terms (that we formally model as local Dirac-delta interactions), of the internal energy of the atomic excited state, and of the coupling terms of the atoms to the laser fields.

Since the loss rate $\hbar\Gamma$ greatly exceeds the kinetic, trapping and interaction energies, we can neglect the external dynamics of the excited state and write

$$\begin{aligned} H \simeq & \int d^3r \sum_{\alpha=a,b}\left[-\frac{\hbar^2}{2m}\hat{\Psi}_\alpha^\dagger\Delta\hat{\Psi}_\alpha + U\hat{\Psi}_\alpha^\dagger\hat{\Psi}_\alpha\right] \\ & + \int d^3r\left[\frac{g_{aa}}{2}\hat{\Psi}_a^{\dagger 2}\hat{\Psi}_a^2 + \frac{g_{bb}}{2}\hat{\Psi}_b^{\dagger 2}\hat{\Psi}_b^2 + g_{ab}\hat{\Psi}_a^\dagger\hat{\Psi}_b^\dagger\hat{\Psi}_b\hat{\Psi}_a\right] \\ & + \int d^3r\,(-\hbar\delta)\hat{\Psi}_e^\dagger\hat{\Psi}_e \\ & + \int d^3r\left[\frac{\hbar\Omega_p}{2}\hat{\Psi}_e^\dagger\hat{\Psi}_a + \frac{\hbar\Omega_c}{2}\hat{\Psi}_e^\dagger\hat{\Psi}_b + \text{h.c.}\right]. \qquad \text{(B2)} \end{aligned}$$

As previously defined, δ is the common value of the detuning of the probe and coupling beams from the $|a\rangle \to |e\rangle$ and $|b\rangle \to |e\rangle$ transitions.

In a Heisenberg picture for the open atomic system, the ground state atomic field operators $\hat{\Psi}_{\alpha=a,b}$ satisfy the usual evolution equations $i\hbar\partial_t\hat{\Psi}_\alpha = [\hat{\Psi}_\alpha, H]$. On the other hand, conservation of the canonical commutation relations of the fields and of the Hermitian conjugation relation between $\hat{\Psi}_\alpha$ and $\hat{\Psi}_\alpha^\dagger$ requires including a quantum Langevin term $\hat{F}_e$ in the evolution equation for the excited state field $\hat{\Psi}_e$,

$$\partial_t\hat{\Psi}_e = \frac{1}{i\hbar}[\hat{\Psi}_e, H] - \frac{1}{2}\Gamma\hat{\Psi}_e + \Gamma^{1/2}\hat{F}_e(\mathbf{r},t)\ . \qquad \text{(B3)}$$

Here, the quantum noise term $\hat{F}_e$ is δ-correlated in position and time, e.g. $[\hat{F}_e(\mathbf{r},t),\hat{F}_e^\dagger(\mathbf{r}',t')] = \delta(\mathbf{r}-\mathbf{r}')\delta(t-t')$, and we recall that the expectation value of normally-ordered products of noise operators vanish, e.g. $\langle\hat{F}_e^\dagger\,\hat{F}_e\rangle = 0$, since the bath does not provide an incoming flux of e atoms.

The only non-zero contributions to the commutator in Eq.(B3) originate from the excited state internal energy and from the atom-laser coupling term. This latter term can be expressed solely in terms of the atomic field operator $\hat{\chi}_{3D}$ in the coupled internal state $|C\rangle$, as defined in Eq.(49). Along the lines of [51], we formally integrate $[\partial_t + (-i\delta + \Gamma/2)]\hat{\Psi}_e = \hat{S}$ neglecting a transient of duration $1/\Gamma$ as

$$\hat{\Psi}_e(\mathbf{r},t) = \int_0^{+\infty} d\tau e^{-(-i\delta+\Gamma/2)\tau}\hat{S}(\mathbf{r},t-\tau). \qquad \text{(B4)}$$

The Rabi frequencies $\Omega_{c,p}$ and the atomic field $\hat{\chi}_{3D}$ have a negligible variation during $1/\Gamma$ and may be replaced by their values at time t in the integrand. This leads to Eq.(50) of the main text, where the noise term is defined as $\hat{B}_e(\mathbf{r},t) = \int_0^{+\infty} d\tau\, e^{-(-i\delta+\Gamma/2)\tau}\hat{F}_e(\mathbf{r},t-\tau)$.

As explained in section III, we are in a regime where the atoms are mostly in the non-coupled state and the

field $\hat{\chi}_{3D}$ in the coupled state is small and a perturbation expansion in powers of $\hat{\chi}_{3D}$ can be performed. The gauge field formalism discussed in Sec.III for the evolution of the atomic field $\hat{\phi}_{3D}$ in the non-coupled state [defined in Eq.(12)] is already recovered at zeroth order in $\hat{\chi}_{3D}$. From this zeroth order approximation of $\hat{\phi}_{3D}$, it is then easy to obtain the first order contribution to the field $\hat{\chi}_{3D}$ that is required in Sec.V to evaluate the optical polarization of the moving atoms.

From Eq.(12) the equation of motion for $\hat{\phi}_{3D}$ is

$$\partial_t \hat{\phi}_{3D} = \frac{1}{i\hbar}[\hat{\phi}_{3D}, H] + \sum_{\alpha=a,b} \hat{\Psi}_\alpha \partial_t \langle NC|\alpha\rangle. \tag{B5}$$

By the very definition of non-coupled state, the excited state internal energy and the atom-laser coupling terms give an exactly vanishing contribution to the commutator. In the rest of the Hamiltonian as well as in the last sum in Eq.(B5), we can perform the approximation $\hat{\Psi}_\alpha \simeq \langle \alpha|NC\rangle \hat{\phi}_{3D}$, which is accurate at zeroth order in $\hat{\chi}_{3D}$. After an integration by part and noting that $\langle NC|\partial_t|NC\rangle$ and $\langle NC|\nabla|NC\rangle$ are purely imaginary quantities, we find that up to this order $\hat{\phi}_{3D}$ follows a purely Hamiltonian evolution governed by Eq.(13).

The equation of motion of $\hat{\chi}_{3D}$ has the form

$$\partial_t \hat{\chi}_{3D} = \frac{1}{i\hbar}[\hat{\chi}_{3D}, H] + \sum_{\alpha=a,b} \hat{\Psi}_\alpha \partial_t \langle C|\alpha\rangle. \tag{B6}$$

The commutator with the internal excited state energy term introduces a $\hat{\Psi}_e$ term, that we replace with Eq.(50): in this way, both a noise term and a complex, position dependent energy term $-(i\delta' + \Gamma'/2)\hat{\chi}_{3D}$ appear in the equation. The real quantities δ' and Γ' are given by Eq.(11) and correspond to lightshift and damping effects, respectively.

Since $\hbar\Gamma'$ is much larger than the kinetic, trapping, interaction and recoil energies of the atoms, we can neglect these latter terms in the evolution equation of the coupled state, and only keep the coupling to $\hat{\phi}_{3D}$. This amounts to keeping in Eq.(B6) only the contributions to the kinetic, trapping and interaction terms of the Hamiltonian H that contain one single factor $\hat{\chi}^\dagger_{3D}$ and an arbitrary number of $\hat{\phi}_{3D}$ and $\hat{\phi}^\dagger_{3D}$ factors. In this way, we obtain

$$\partial_t \hat{\chi}_{3D} \simeq -(i\delta' + \frac{\Gamma'}{2})\hat{\chi}_{3D} + \hat{\phi}_{3D}\langle C|[-\partial_t + \frac{i\hbar}{2m}\Delta]|NC\rangle + \frac{i\hbar}{m}\nabla\hat{\phi}_{3D}\cdot\langle C|\nabla|NC\rangle + \frac{1}{i\hbar}\mathcal{G}\hat{\phi}^\dagger_{3D}\hat{\phi}^2_{3D} + \Gamma'^{1/2}\hat{F}_\chi \tag{B7}$$

where we have introduced a complex position and time dependent coupling constant

$$\mathcal{G} = \langle C|a\rangle\langle a|NC\rangle[(g_{aa} - g_{ab})\langle NC|a\rangle\langle a|NC\rangle - a \leftrightarrow b] \tag{B8}$$

with the convention $g_{ba} = g_{ab}$. The noise term is defined by $\hat{F}_\chi = -i|\delta + i\Gamma/2|(\Omega_c^*/|\Omega_c|)\hat{B}_e$. Its correlation properties are determined by the commutation relation $[\hat{F}_\chi(\mathbf{r},t), \hat{F}^\dagger_\chi(\mathbf{r}',t')] \simeq \frac{|\delta+i\Gamma/2|^2}{\Gamma} e^{i(t-t')\delta - \Gamma|t-t'|/2}\delta(\mathbf{r}-\mathbf{r}')$. Since we are working in a low saturation regime in which $\Gamma \gg \Gamma'$, the time dependent factor in front of $\delta(\mathbf{r}-\mathbf{r}')$ may be replaced with a Dirac of $t-t'$, so that $\hat{F}_\chi$ is in practice a spatio-temporally delta-correlated noise.

The last step is to expand Eq.(B7) to first order in Ω_p/Ω_c. Then (i) for $g_{aa} \simeq g_{ab}$, the last contribution in the right-hand side of Eq.(B7) vanishes [68], and (ii) for the magic choice Eq.(23), the third contribution vanishes. With the same adiabatic elimination technique adopted for $\hat{\Psi}_e$ and taking into account the fact that δ' and Γ' vary very slowly on the scale of $1/\Gamma'$, we are finally led to the final equation Eq.(52) with a noise term defined by $\hat{B}_\chi(\mathbf{r},t) = \int_0^{+\infty} d\tau e^{-[i\delta' + \Gamma'/2](\mathbf{r},t)\tau}\hat{F}_\chi(\mathbf{r},t-\tau)$.

We complete the discussion by giving the back-action of the field $\hat{\chi}_{3D}$ on the field $\hat{\phi}_{3D}$, a back-action that was already considered for a specific single atom geometry in [43]. The linear coupling of $\hat{\phi}_{3D}$ to $\hat{\chi}_{3D}$ originates from terms in the Hamiltonian that are linear in $\hat{\chi}_{3D}$, leading to

$$\left(\partial_t\hat{\phi}_{3D}\right)_{\rm back} = \hat{\chi}_{3D}\langle NC|[-\partial_t + \frac{i\hbar}{2m}\Delta]|C\rangle + \frac{i\hbar}{m}\nabla\hat{\chi}_{3D}\cdot\langle NC|\nabla|C\rangle + \frac{1}{i\hbar}[\mathcal{G}\hat{\chi}^\dagger_{3D}\hat{\phi}^2_{3D} + 2\mathcal{G}^*\hat{\phi}^\dagger_{3D}\hat{\phi}_{3D}\hat{\chi}_{3D}]. \tag{B9}$$

Expression of the back-action solely in terms of $\hat{\phi}_{3D}$ and noise operators is obtained by replacing $\hat{\chi}_{3D}$ in the resulting equations of motion with its adiabatic approximation derived from Eq.(B7). This leads in general to a lengthy formula. For simplicity, we give the result to leading order in Ω_p/Ω_c for $g_{aa} = g_{ab}$, we neglect the contribution to $\langle C|\partial_t|NC\rangle$ of the time-dependence of the switch-off function $f(t)$, and we use the specific form Ω_p/Ω_c considered in this paper, so that

$$\left(\partial_t\hat{\phi}_{3D}\right)_{\rm back} \simeq -\frac{i\hbar^2}{m^2}\frac{4(\delta+i\Gamma/2)}{|\Omega_c|^2}\left|\frac{\Omega_p}{\Omega_c}\right|^2 \times \times [(\mathbf{k}_p - \mathbf{k}_c)\cdot\nabla]^2\,\hat{\phi}_{3D} + \text{noise terms}. \tag{B10}$$

After reduction to the xy plane, the deterministic term gives rise to two corrections to the evolution of $\hat{\phi}_{3D}$: (i) a complex position dependent energy shift,

$$\hbar(\delta'' - i\Gamma''/2) = -2(\delta + i\Gamma/2)\omega_z\frac{\hbar^2k_c^2}{m}\frac{|\Omega_p|^2}{|\Omega_c|^4}, \tag{B11}$$

and (ii) a complex correction to the mass along y, $\delta m_y = 8\hbar k_c^2|\Omega_p|^2(\delta + i\Gamma/2)/|\Omega_c|^4$. $\hbar\delta''$ is the lightshift potential experienced by the non-coupled bidimensional field. The spatial average of the fluorescence rate Γ'' of the non-coupled field coincides with the $\Gamma^{\rm non-ad}_{\rm fluo}$ fluorescence rate previously discussed in (A2), as it should be. For the parameters of Table I, the reactive corrections δ'' and δm_y are small provided that the detuning is not too large, $|\delta/\Gamma| < 5$. For instance, an estimate for the energy deposited by the $\hbar\delta''$ potential can be obtained from the Bogoliubov theory for a homogeneous system, see Eq.(D15),

leading to

$$\frac{\Delta E_{\hbar\delta''}}{\Delta E_2} \approx \frac{5\cdot 10^{-5}}{f_n}(\delta/\Gamma)^2. \quad \text{(B12)}$$

Appendix C: Derivation of the expression for the deposited energy

We start from a two-dimensional system at thermal equilibrium with no average current and we apply a gauge field of the form

$$\mathbf{A}(\mathbf{r},t) = f(t)\mathbf{e}_y |c_+ e^{i\mathbf{q}\cdot\mathbf{r}/2} + c_- e^{-i\mathbf{q}\cdot\mathbf{r}/2}|^2 e^{-(\mathbf{r}-\mathbf{r}_0)^2/(2\sigma^2)}, \quad \text{(C1)}$$

where $\mathbf{e}_\alpha$ is the unit vector along direction α. The derivable dimensionless envelope function $f(t)$ is assumed to be zero for $t<0$ and to rapidly tend to zero for $t\to+\infty$. The coefficients $c_\pm$ have the dimension of the square root of a momentum.

We are interested in evaluating the energy change of the system from $t=0^-$ to $t=+\infty$ at the lowest order in $c_\pm$. We work in Schrödinger picture and we first use the exact relations:

$$\Delta E \equiv \int_{-\infty}^{+\infty} dt \frac{d\langle H(t)\rangle}{dt} \quad \text{(C2)}$$

$$= \int_{-\infty}^{+\infty} dt \int d^2r \mathbf{A}(\mathbf{r},t)\cdot\frac{d}{dt}\langle \mathbf{j}(\mathbf{r})\rangle(t), \quad \text{(C3)}$$

where the second equality comes from a time-dependent Hellmann-Feynman theorem and a temporal integration by parts. Calculating $\langle \mathbf{j}(\mathbf{r})\rangle(t)$ by linear response theory gives

$$\Delta E \simeq \int_{\mathbb{R}} \frac{d\omega}{2\pi}\int d^2r \int d^2r'\,\omega \, \mathrm{Im}\left[\sum_{\alpha,\beta}\chi^{\mathrm{ex}}_{\alpha\beta}(\mathbf{r},\mathbf{r}';\omega)A_\alpha(\mathbf{r},\omega)^* A_\beta(\mathbf{r}',\omega)\right], \quad \text{(C4)}$$

where χ^{ex} is the exact current susceptibility in real space taking into account the spatial inhomogeneity of the trapped cloud. Note that, contrarily to Eq.(C2), Eqs.(C3),(C4) still hold when $f(t)=0$ for $t<0$ and has a discontinuous jump in $t=0$.

We now use the particular form (C1) for $\mathbf{A}$ and consider the relevant limiting case $q\sigma\gg 1$, $q\min(\xi,\lambda)\ll 1$, where ξ is the healing length of the gas and λ is the thermal de Broglie wavelength. We also assume that σ is much smaller than the radius of the trapped cloud, so that the density variation within a region of radius σ around $\mathbf{r}_0$ may be neglected.

Within a local density approximation, we then replace χ^{ex} with the susceptibility χ of a spatially homogeneous system with a density equal to the one of the trapped gas at position $\mathbf{r}_0$ and with the same temperature, $\chi^{\mathrm{ex}}(\mathbf{r},\mathbf{r}';\omega)\simeq\chi(\mathbf{r}-\mathbf{r}';\omega)$.

This local density approximation leads to

$$\Delta E \simeq \int_{\mathbb{R}}\frac{d\omega}{2\pi}\omega\,|f(\omega)|^2\int d^2R\int d^2u\,\Big[|c_+|^2+|c_-|^2 + c_+^* c_- e^{-i\mathbf{q}\cdot(\mathbf{R}+\mathbf{u}/2)} + c_+ c_-^* e^{i\mathbf{q}\cdot(\mathbf{R}+\mathbf{u}/2)}\Big]\Big[|c_+|^2+|c_-|^2 + c_+^* c_- e^{-i\mathbf{q}\cdot(\mathbf{R}-\mathbf{u}/2)} + c_+ c_-^* e^{i\mathbf{q}\cdot(\mathbf{R}-\mathbf{u}/2)}\Big] \mathrm{Im}[\chi_{yy}(\mathbf{u};\omega)]\, e^{-|\mathbf{R}-\mathbf{r}_0|^2/\sigma^2} e^{-u^2/(4\sigma^2)} \quad \text{(C5)}$$

where we have performed the change of variables $\mathbf{r}=\mathbf{R}+\mathbf{u}/2, \mathbf{r}'=\mathbf{R}-\mathbf{u}/2$. As we work in the $q\sigma\gg 1$ regime, we have for example

$$\int d^2R\, e^{-2i\mathbf{q}\cdot\mathbf{R}}\, e^{-|\mathbf{R}-\mathbf{r}_0|^2/\sigma^2} = e^{-2i\mathbf{q}\cdot\mathbf{R}_0}\,\pi\sigma^2\, e^{-q^2\sigma^2} \ll \pi\sigma^2 \quad \text{(C6)}$$

so that all the oscillating terms in $\mathbf{R}$ may be neglected. Introducing the Fourier transform of $\chi_{yy}(\mathbf{k};\omega)$, which is an even function of $\mathbf{k}$ due to parity or rotational invariance, we obtain

$$\Delta E = \Delta E_1 + \Delta E_2 \quad \text{(C7)}$$

$$\Delta E_1 \simeq \int_{-\infty}^{+\infty}\frac{d\omega}{2\pi}\omega|f(\omega)|^2(2\pi\sigma^2)^2\int\frac{d^2k}{(2\pi)^2} \mathrm{Im}\,\chi_{yy}(\mathbf{k};\omega)\left(|c_+|^2+|c_-|^2\right)^2 e^{-k^2\sigma^2} \quad \text{(C8)}$$

$$\Delta E_2 \simeq \int_{-\infty}^{+\infty}\frac{d\omega}{2\pi}\omega|f(\omega)|^2(2\pi\sigma^2)^2\int\frac{d^2k}{(2\pi)^2} \mathrm{Im}\,\chi_{yy}(\mathbf{q}+\mathbf{k};\omega)2|c_+|^2|c_-|^2 e^{-k^2\sigma^2}. \quad \text{(C9)}$$

The second contribution ΔE_2 comes from the spatially modulated gauge field at $\mathbf{q}$, while the first contribution ΔE_1 is due to the non-modulated term which follows the broad Gaussian envelope. The expression (24) in the main text is obtained from (C9) by noting that the integration over $\mathbf{k}$ is effectively limited by the Gaussian factor to a small region of radius $1/\sigma$ in which one is allowed to neglect the $\mathbf{k}$-dependence of the susceptibility.

Naively, one could guess that a necessary condition for the accuracy of our local density approximation is that the duration in time of the gauge field γ^{-1} is short as compared to the characteristic time R/v for the induced mechanical perturbation to explore the whole cloud, v being the fastest between the sound and thermal speeds in the cloud of radius R.

This condition is actually sufficient, but not necessary within linear response theory. We now show for $f(t)=\Theta(t)e^{-\gamma t}$ that the $\gamma\to 0$ limit for the deposited energy scheme exists and coincides with the perturbation induced by the gauge field in the thermodynamical equilibrium state. As one can show by inserting the explicit form of the temporal Fourier transform of the gauge field into (C4) and performing the integral over ω, the de-

posited energy can be written in the form

$$\Delta E \simeq \frac{1}{2}\mathrm{Re}\Big[\int d^2r\, d^2r' \sum_{\alpha,\beta} A_\alpha(\mathbf{r}, t=0^+) \\ A_\beta(\mathbf{r}', t=0^+)\, \chi^{\rm ex}_{\alpha\beta}(\mathbf{r},\mathbf{r}';\omega=i\gamma)\Big] \quad \text{(C10)}$$

where we have introduced the Kubo formula for the exact current-current susceptibility

$$\chi^{\rm ex}_{\alpha\beta}(\mathbf{r},\mathbf{r}';\omega) = \sum_{\lambda,\lambda'} (\pi_\lambda - \pi_{\lambda'}) \frac{\langle\lambda|j_\alpha(\mathbf{r})|\lambda'\rangle\langle\lambda'|j_\beta(\mathbf{r}')|\lambda\rangle}{E_{\lambda'} - E_\lambda - \hbar\omega - i0^+} \quad \text{(C11)}$$

in terms of the thermal equilibrium population π_λ of quantum state λ. This quantity can be simply related to the susceptibility at thermodynamical equilibrium,

$$\chi^{\rm th}_{\alpha\beta}(\mathbf{r},\mathbf{r}') = \lim_{\gamma\to 0} \mathrm{Re}[\chi^{\rm ex}_{\alpha\beta}(\mathbf{r},\mathbf{r}';\omega=i\gamma)] + \\ + \frac{1}{k_B T} \sum_{\lambda,\lambda';E_\lambda=E_{\lambda'}} \pi_\lambda \langle\lambda|j_\alpha(\mathbf{r})|\lambda'\rangle\langle\lambda'|j_\beta(\mathbf{r}')|\lambda\rangle. \quad \text{(C12)}$$

We recall that the thermodynamic susceptibility relates the mean current in a thermal equilibrium state at temperature T to the applied (weak) static gauge field via $\langle\mathbf{j}\rangle = \chi^{\rm th} * \mathbf{A}$, where $*$ is the convolution product. In the present case of an interacting gas, one can safely expect that the second line in (C12) gives a negligible contribution as there is no systematic degeneracy and the current operator $\mathbf{j}$ has no diagonal matrix elements since the eigenstate wavefunctions may be taken real.

Since application of local density approximation in the thermodynamical equilibrium state is a standard procedure, we expect that within linear response theory our deposited energy method is accurately described by a local density approximation down to the $\gamma \to 0$ limit.

Appendix D: Some results of linear response theory and the Bogoliubov expression of the deposited energy

A system of time independent Hamiltonian H_0 experiences, at times $t > 0$, a time dependent weak perturbation of Hamiltonian $-\epsilon f(t)\mathcal{V}$, where $\epsilon \to 0$, the dimensionless time dependent factor $f(t)$ is zero for $t < 0$ and tends rapidly to zero for $t \to +\infty$, and the operator $\mathcal{V}$ is time independent. At time $t = +\infty$, the system is free again, with a mean energy modified by the perturbation. The question is to calculate the mean energy change to second order in ϵ.

Suppose first that, at $t = 0^-$, the system is prepared in the eigenstate $|\lambda\rangle$ of H_0 of eigenenergy E_λ. The energy change δE between time 0 and time $+\infty$ is

$$\delta E = \lim_{t\to+\infty} \langle\psi(t)|(H_0 - E_\lambda)|\psi(t)\rangle \quad \text{(D1)}$$

where $|\psi(t)\rangle$ is the system state vector at time t. The usual time dependent perturbation theory gives an expansion in powers of ϵ:

$$|\psi(t)\rangle = |\psi_0(t)\rangle + \epsilon|\psi_1(t)\rangle + \epsilon^2|\psi_2(t)\rangle + \ldots \quad \text{(D2)}$$

where $|\psi_0(t)\rangle = \exp(-iE_\lambda t/\hbar)|\lambda\rangle$,

$$|\psi_1(t)\rangle = -\int_0^t \frac{d\tau}{i\hbar} e^{-iH_0(t-\tau)/\hbar} f(\tau)\mathcal{V} e^{-iE_\lambda\tau/\hbar}|\lambda\rangle, \quad \text{(D3)}$$

and the expression of higher order contributions is not needed. Using $(H_0 - E_\lambda)|\psi_0(t)\rangle = 0$ and $\langle\psi_0(t)|(H_0 - E_\lambda) = 0$, we find to second order in ϵ:

$$\delta E \simeq \lim_{t\to+\infty} \epsilon^2 \langle\psi_1(t)|(H_0 - E_\lambda)|\psi_1(t)\rangle. \quad \text{(D4)}$$

In this paper, $f(t) = Y(t)\exp(-\gamma t)$, with $\gamma > 0$ and $Y(t)$ be Heavyside step function Also, the system is prepared initially in a statistical mixture of eigenstates of H_0 with a probability distribution π_λ. After explicit integration of (D3) over τ and then average over $|\lambda\rangle$, the expression for the signal to be detected experimentally is

$$\mathrm{Signal}\,(\mathcal{V}) \equiv \lim_{\epsilon\to 0} \frac{\langle\delta E\rangle}{\epsilon^2} = \\ \frac{1}{2}\,\mathrm{Re} \sum_{\lambda,\lambda'} \frac{(\pi_\lambda - \pi_{\lambda'})}{E_{\lambda'} - E_\lambda - i\hbar\gamma} |\langle\lambda'|\mathcal{V}|\lambda\rangle|^2. \quad \text{(D5)}$$

The sum may be restricted to $E_\lambda \neq E_{\lambda'}$ since the contributions with $E_\lambda = E_{\lambda'}$ are zero. This also shows that the signal has a finite limit for $\gamma \to 0^+$. Note that in a thermal equilibrium state $\pi_\lambda = Z^{-1}\exp(-E_\lambda/k_B T)$, the signal is necessarily positive.

The calculation of the noise on the experimental signal can be performed along the same lines. One defines $\delta E^2 \equiv \lim_{t\to+\infty}\langle\psi(t)|(H_0 - E_\lambda)^2|\psi(t)\rangle$ with the initial state vector $|\psi(0)\rangle = |\lambda\rangle$, and one finds after average over the initial state:

$$[\mathrm{Noise}\,(\mathcal{V})]^2 \equiv \lim_{\epsilon\to 0} \frac{\langle\delta E^2\rangle}{\epsilon^2} \underset{\gamma\to 0}{=} \sum_{\lambda,\lambda',E_\lambda\neq E'_\lambda} \pi_\lambda |\langle\lambda|\mathcal{V}|\lambda'\rangle|^2 \simeq \\ \sum_\lambda \pi_\lambda [\langle\lambda|\mathcal{V}^2|\lambda\rangle - \langle\lambda|\mathcal{V}|\lambda\rangle^2], \quad \text{(D6)}$$

where the approximate equality is based on the assumption that there are no systematic degeneracies in the many-body spectrum. The ϵ^2 scaling of the variance in Eq.(D6) shows that the typical value of the energy change at the end of the excitation sequence is of order ϵ. This scaling is to be contrasted with the ϵ^2 one of the expectation value that is suggested by Eq.(D5).

We now apply the general formula Eq.(D5) to the Bogoliubov analysis of subsection IV B. In this case, $\epsilon = \epsilon_{\rm gauge}/2$ and $\mathcal{V} = \mathcal{V}_q + \mathcal{V}_{-q}$ with

$$\mathcal{V}_q = \int_{[0,L]^2} d^2r\, e^{iqx} j_y(\mathbf{r}) = \sum_{\mathbf{k}} \frac{\hbar k_y}{m} a^\dagger_{\mathbf{k}+\mathbf{q}} a_{\mathbf{k}} \quad \text{(D7)}$$

where $a_{\mathbf{k}}$ is the annihilation operator of a particle of the gas of wavevector $\mathbf{k}$, and we have set $\mathbf{q} = q\mathbf{e}_x$. In a translationally invariant system, the eigenstates $|\lambda\rangle$ can be taken of well defined total momentum; as the action of $\mathcal{V}_{\pm q}$ changes this total momentum by $\pm\hbar\mathbf{q}$, the two operators $\mathcal{V}_q$ and $\mathcal{V}_{-q}$ cannot interfere in the signal and thus $\text{Signal}\,(\mathcal{V}) = 2\,\text{Signal}\,(\mathcal{V}_q)$. In terms of the annihilation operators $b_{\mathbf{k}}$ of Bogoliubov quasiparticles, we can split

$$\mathcal{V}_q = \mathcal{V}_q^{(0)} + \mathcal{V}_q^{(2)} + \mathcal{V}_q^{(-2)} \tag{D8}$$

in terms of

$$\mathcal{V}_q^{(0)} = \sum_{\mathbf{k}\neq\mathbf{0},-\mathbf{q}} \frac{\hbar k_y}{m}(U_{\mathbf{k}}U_{\mathbf{k}+\mathbf{q}} - V_{\mathbf{k}}V_{\mathbf{k}+\mathbf{q}})\, b^\dagger_{\mathbf{k}+\mathbf{q}} b_{\mathbf{k}} \tag{D9}$$

$$\mathcal{V}_q^{(2)} = {\sum_{\mathbf{k}\neq\mathbf{0},-\mathbf{q}}}' \frac{\hbar k_y}{m}(V_{\mathbf{k}}U_{\mathbf{k}+\mathbf{q}} - U_{\mathbf{k}}V_{\mathbf{k}+\mathbf{q}})\, b^\dagger_{\mathbf{k}+\mathbf{q}} b^\dagger_{-\mathbf{k}} \tag{D10}$$

$$\mathcal{V}_q^{(-2)} = {\sum_{\mathbf{k}\neq\mathbf{0},-\mathbf{q}}}' \frac{\hbar k_y}{m}(U_{\mathbf{k}}V_{\mathbf{k}+\mathbf{q}} - V_{\mathbf{k}}U_{\mathbf{k}+\mathbf{q}})\, b_{\mathbf{k}} b_{-(\mathbf{k}+\mathbf{q})}. \tag{D11}$$

The primed sum $\sum'$ indicates restriction of the sum over wavevectors such that $k_y > 0$. In Bogoliubov theory, the eigenstates $|\lambda\rangle$ may be taken in the form of Fock states of quasiparticles. Since $\mathcal{V}_q^{(n)}$ changes the total number of quasiparticles by the amount n, the terms in the right hand side of Eq.(D8) cannot interfere in the signal and

$$\text{Signal}\,(\mathcal{V}_q) = \text{Signal}\,(\mathcal{V}_q^{(0)}) + \text{Signal}\,(\mathcal{V}_q^{(2)}) + \text{Signal}\,(\mathcal{V}_q^{(-2)}). \tag{D12}$$

Thanks to the clever writing of $\mathcal{V}_q^{(n)}$ with the constraint $k_y > 0$ [52], there are no interferences in Eqs.(D9,D10,D11) between the different terms of the sums over $\mathbf{k}$. As a result, the whole signal is the sum over the contribution of the different $\mathbf{k}$'s. The last trick is to express the ratios $\pi_{\lambda'}/\pi_\lambda$ in terms of the mean occupation numbers $n_{\mathbf{k}}$ of the Bogoliubov modes of energy $\epsilon_{\mathbf{k}}$ and to make use of the identity

$$e^{\beta\epsilon_{\mathbf{k}}} = \frac{n_{\mathbf{k}}+1}{n_{\mathbf{k}}} \tag{D13}$$

satisfied by the Bose law. A little bit of rewriting taking advantage of the relation $\text{Signal}(\mathcal{V}) = (N/m) f_n^{\text{eff}}$ and of the remarks in [52], finally leads to Eq.(30).

An alternative procedure is to calculate the current-current susceptibility (C11) for a spatially homogeneous system within the Bogoliubov theory, which for $\mathbf{q} \perp \mathbf{e}_y$ gives in dimension d:

$$\begin{aligned}\chi_{yy}(\mathbf{q};\omega) = \frac{1}{L^d}\sum_{\mathbf{k}\neq 0,-\mathbf{q}} \frac{\hbar^2 k_y^2}{m^2} \\ \Big[\frac{n_{\mathbf{k}} - n_{\mathbf{k}+\mathbf{q}}}{\epsilon_{\mathbf{k}+\mathbf{q}} - \epsilon_{\mathbf{k}} - \hbar\omega - i0^+}\left(U^2_{\mathbf{k}+\mathbf{q}}U^2_{\mathbf{k}} - U_{\mathbf{k}+\mathbf{q}}V_{\mathbf{k}+\mathbf{q}}U_{\mathbf{k}}V_{\mathbf{k}}\right) \\ -\frac{1+n_{\mathbf{k}}+n_{\mathbf{k}+\mathbf{q}}}{-\epsilon_{\mathbf{k}+\mathbf{q}} - \epsilon_{\mathbf{k}} - \hbar\omega - i0^+}\left(V^2_{\mathbf{k}+\mathbf{q}}U^2_{\mathbf{k}} - U_{\mathbf{k}+\mathbf{q}}V_{\mathbf{k}+\mathbf{q}}U_{\mathbf{k}}V_{\mathbf{k}}\right) \\ +\frac{1+n_{\mathbf{k}}+n_{\mathbf{k}+\mathbf{q}}}{\epsilon_{\mathbf{k}+\mathbf{q}} + \epsilon_{\mathbf{k}} - \hbar\omega - i0^+}\left(U^2_{\mathbf{k}+\mathbf{q}}V^2_{\mathbf{k}} - U_{\mathbf{k}+\mathbf{q}}V_{\mathbf{k}+\mathbf{q}}U_{\mathbf{k}}V_{\mathbf{k}}\right) \\ +\frac{n_{\mathbf{k}+\mathbf{q}} - n_{\mathbf{k}}}{\epsilon_{\mathbf{k}} - \epsilon_{\mathbf{k}+\mathbf{q}} - \hbar\omega - i0^+}\left(V^2_{\mathbf{k}+\mathbf{q}}V^2_{\mathbf{k}} - U_{\mathbf{k}+\mathbf{q}}V_{\mathbf{k}+\mathbf{q}}U_{\mathbf{k}}V_{\mathbf{k}}\right)\Big].\end{aligned} \tag{D14}$$

From Eq.(C4) one then recovers expression Eq.(30) for the effective normal fraction f_n^{eff}.

Another application of Eq.(D5) is to calculate the energy deposited by the external potential $\mathcal{U}(\mathbf{r},t) = (\mathcal{U}_0 e^{i\mathbf{Q}\cdot\mathbf{r}} + \text{c.c})\Theta(t)e^{-\eta t}$ in the spatially homogeneous case. This is useful for Appendix A and Appendix B to estimate the effect of undesired lightshifts. In second quantized form, and to leading order in Bogoliubov theory, one then has $\epsilon\mathcal{V} = N^{1/2}(U_Q + V_Q)[\mathcal{U}_0(b^\dagger_{\mathbf{Q}} + b_{-\mathbf{Q}}) + \text{h.c.}]$. These terms do not interfer in Eq.(D5). For non-zero temperature, using (D13), we then obtain a temperature independent result

$$\Delta E_{\mathcal{U}} \simeq 2N|\mathcal{U}_0|^2(U_Q + V_Q)^2\,\text{Re}\,\frac{1}{\epsilon_Q - i\hbar\eta} \tag{D15}$$

Remarkably, this also allows to calculate the energy change ΔE_g due to the switch-on-and-off of a spatially modulated coupling constant, $\delta g(\mathbf{r},t) = (\delta g_0 e^{i\mathbf{q}\cdot\mathbf{r}} + \text{c.c.})\Theta(t)e^{-\gamma t}$. For a spatially homogeneous system, to leading order of Bogoliubov theory, the relevant operator is $\epsilon\mathcal{V} = N^{1/2}(U_q + V_q)[\rho\delta g_0(b^\dagger_{\mathbf{q}} + b_{-\mathbf{q}}) + \text{h.c.}]$, so that one can formally apply Eq.(D15) with $\mathcal{U}_0 = \rho\delta g_0$. This can be applied to the variation of the coupling constant due to $g_{aa} \neq g_{ab}$ in Eq.(18). In this case $\delta g_0 = 2g[(g_{ab} - g_{aa})/g_{aa}](\Omega_p^+\Omega_p^{-*})(0^+)/|\Omega_c|^2$ so that for $q\xi = 1$ and $\gamma \to 0$,

$$\frac{\Delta E_g}{\Delta E_2} \simeq \frac{16}{5 f_n}\frac{m\rho g}{(\hbar k_c)^2}\left(\frac{g_{ab} - g_{aa}}{g_{aa}}\right)^2. \tag{D16}$$

For the values of Table I and $|g_{ab} - g_{aa}| \lesssim 0.1|g_{aa}|$ as expected for ^{87}Rb, this gives $\Delta E_g/\Delta E_2 \approx 7\cdot 10^{-4}/f_n$ which is negligible.

[1] V. L. Berezinskii, Zh. Eksp. Teor. Fiz. **61**, 1144 (1971) [Sov. Phys. JETP 34, 610 (1972)]; J. M. Kosterlitz and D. J. Thouless, J. Phys. C **5**, L124 (1972); J. M. Kosterlitz and D. J. Thouless, J. Phys. C **6**, 1181 (1973); J. M. Kosterlitz, J. Phys. C **7**, 1047 (1974).

[2] P. Minnhagen, Rev. Mod. Phys. **59**, 1001 (1987).

[3] M. Chester and L. C. Yang, Phys. Rev. Lett. **31**, 1377 (1973); D. J. Bishop and J. D. Reppy, Phys. Rev. Lett. **40**, 1727 (1978).

[4] Z. Hadzibabic, P. Krüger, M. Cheneau, B. Battelier, and

J. Dalibard, Nature **441**, 1118 (2006).
[5] V. Schweikhard, S. Tung, and E. A. Cornell, Phys. Rev. Lett. **99**, 030401 (2007).
[6] P. Cladé, C. Ryu, A. Ramanathan, K. Helmerson, and W. D. Phillips, Phys. Rev. Lett. **102**, 170401 (2009).
[7] I. Carusotto, Physics **3**, 5 (2010).
[8] N. R. Cooper and Z. Hadzibabic, Phys. Rev. Lett. **104**, 030401 (2010); S. T. John, Z. Hadzibabic, N. R. Cooper, preprint arXiv:1011.2532.
[9] T.-L. Ho, Q. Zhou, Nature Phys. **6**, 131 (2009).
[10] S. P. Rath, T. Yefsah, K. J. Günter, M. Cheneau, R. Desbuquois, M. Holzmann, W. Krauth, and J. Dalibard, Phys. Rev. A **82**, 013609 (2010).
[11] K.W. Madison, F. Chevy, W. Wohlleben, and J. Dalibard, Phys. Rev. Lett. **84**, 806 (2000); K. Madison, F. Chevy, V. Bretin, and J. Dalibard, Phys. Rev. Lett. **86**, 4443 (2001).
[12] S. Sinha, Y. Castin, Phys. Rev. Lett. **87**, 190402 (2001).
[13] C. Lobo, A. Sinatra, Y. Castin, Phys. Rev. Lett. **92**, 020403 (2004); N.G. Parker, C.S. Adams, Phys. Rev. Lett. **95**, 145301 (2005); N.G. Parker, C.S. Adams, J. Phys B **39**, 43 (2006).
[14] D. Pines and P. Nozières, *The Theory of Quantum Liquids* (Benjamin, New York, 1966), Vol. I; P. Nozières and D. Pines, *The Theory of Quantum Liquids* (Addison-Wesley, Reading, MA, 1990), Vol. II.
[15] F. Dalfovo and S. Stringari, Phys. Rev. B **46**, 13991 (1992)
[16] R. Dum and M. Olshanii, Phys. Rev. Lett. **76**, 1788 (1996).
[17] F. Gerbier and J. Dalibard, New J. Phys. **12**, 033007 (2010).
[18] A. Robert, O. Sirjean, A. Browaeys, J. Poupard, S. Nowak, D. Boiron, C. I. Westbrook, and A. Aspect, Science, **292**, 461 (2001).
[19] F. Pereira Dos Santos, J. Léonard, Junmin Wang, C. J. Barrelet, F. Perales, E. Rasel, C. S. Unnikrishnan, M. Leduc, and C. Cohen-Tannoudji Phys. Rev. Lett. **86**, 3459 (2001).
[20] Y.-J. Lin, R. L. Compton, A. R. Perry, W. D. Phillips, J. V. Porto, and I. B. Spielman, Phys. Rev. Lett. **102**, 130401 (2009).
[21] Y.-J. Lin, R. L. Compton, K. Jiménez-García, J. V. Porto, I. B. Spielman, Nature **462**, 628 (2009).
[22] T.L. Ho, Phys. Rev. Lett. **81**, 742 (1998); W. Zhang and D.F Walls, Phys. Rev. A **57**, 1248 (1998); T. Ohmi and K. Machida, J. Phys. Soc. Jpn. **67**, 1822 (1998).
[23] Y. Castin, C. Herzog, Comptes Rendus de l'Académie des Sciences de Paris, tome 2, série IV, p.419 (2001).
[24] T. Stöferle, H. Moritz, C. Schori, M. Köhl, T. Esslinger, Phys. Rev. Lett. **92**, 130403 (2004); M. Krämer, C. Tozzo, F. Dalfovo, Phys. Rev. A **71**, R061602 (2005); I. Carusotto, R. Balbinot, A. Fabbri, A. Recati, Eur. Phys. J. D **56**, 391 (2010).
[25] C. W. Gardiner, P. Zoller, *Quantum Noise* (Springer, 2004).
[26] J. Dalibard, F. Gerbier, G. Juzeliunas, P. Öhberg, preprint arXiv:1008.5378.
[27] In the configurations shown in Fig.6, only the case $\alpha = \pi/2$ is realized. To obtain $\alpha = 0$ with the first choice of level scheme, one may e.g. choose a sublevel $|b\rangle = |F = 2, m_F = -1\rangle$ and take the coupling beam propagating along x with a linear polarization along y.
[28] The apparent agreement of this value $f_n \simeq 0.22$ obtained from a quantum Bogoliubov calculation with the result of the classical field simulation of Fig.3 for $T/T_d = 0.1$ is accidental. A Bogoliubov calculation for the classical field would give a 40% deviation from this value.
[29] Yu. Kagan, B. V. Svistunov, and G. V. Shlyapnikov, Sov. Phys. JETP **75**, 387 (1992); Yu. Kagan and B. V. Svistunov, Phys. Rev. Lett. **79**, 3331 (1997); N. G. Berloff and B. V. Svistunov, Phys. Rev. A **66**, 013603 (2002); K. Damle, M. J. Davis, S.A. Morgan and K. Burnett, Phys. Rev. Lett. **87**, 160402 (2001); K. Góral, M. Gajda, K. Rzążewski, Opt. Express **8**, 92 (2001); D. Kadio, M. Gajda and K. Rzążewski, Phys. Rev. A **72**, 013607 (2005); A. Sinatra, Y. Castin, and E. Witkowska, Phys. Rev. A **75**, 033616 (2007); A. Sinatra, Y. Castin, and E. Witkowska, Phys. Rev. A **80**, 033614 (2009).
[30] E. Mandonnet, Ph.D. thesis, University Paris 6 (2000); [http://tel. archives-ouvertes.fr/tel-00011872/fr/].
[31] A. Sinatra, Y. Castin, and Yun Li, Phys. Rev. A **81**, 053623 (2010); K. Maussang, G. Edward Marti, T. Schneider, P. Treutlein, Yun Li, A. Sinatra, R. Long, J. Estève, and J. Reichel, Phys. Rev. Lett. **105**, 080403 (2010).
[32] A. J. Leggett, Rev. Mod. Phys. **71**, S318 (1999).
[33] I. Carusotto and Y. Castin, Comptes Rendus Physique **5**, 107 (2004).
[34] N. Prokof'ev, O. Ruebenacker, and B. Svistunov, Phys. Rev. Lett. **87**, 270402 (2001).
[35] M. Greiner, C. A. Regal, J. T. Stewart, and D. S. Jin, Phys. Rev. Lett. **94**, 110401 (2005); S. Fölling, F. Gerbier, A. Widera, O. Mandel, T. Gericke, I. Bloch, Nature **434**, 481 (2005); T. Rom, Th. Best, D. van Oosten, U. Schneider, S. Fölling, B. Paredes and I. Bloch, Nature **444**, 733 (2006); A. Perrin, H. Chang, V. Krachmalnicoff, M. Schellekens, D. Boiron, A. Aspect, and C. I. Westbrook, Phys. Rev. Lett. **99**, 150405 (2007); T. Jeltes, J. M. McNamara, W. Hogervorst, W. Vassen, V. Krachmalnicoff, M. Schellekens, A. Perrin, H. Chang, D. Boiron, A. Aspect, and C. I. Westbrook, Nature **445**, 402 (2007); S. Hofferberth, I. Lesanovsky, T. Schumm, A. Imambekov, V. Gritsev, E. Demler, J. Schmiedmayer, Nature Phys. **4**, 489 (2008).
[36] E. Altman, E. Demler, and M. D. Lukin, Phys. Rev. A **70**, 013603 (2004); I. Carusotto and Y. Castin, Phys. Rev. Lett. **94**, 223202 (2005); V. Gritsev, E. Altman, E. Demler, and A. Polkovnikov, Nature Phys. **2**, 705 (2006); I. Carusotto, S. Fagnocchi, A. Recati, R. Balbinot, and A. Fabbri, New J. Phys. **10**, 103001 (2008).
[37] L.P. Pitaevskii and S. Stringari, *Bose-Einstein Condensation*, Clarendon Press Oxford (2003).
[38] M. Fleischhauer, A. Imamoglu, and J. P. Marangos, Rev. Mod. Phys. **77**, 633 (2005).
[39] L.V. Hau, S.E. Harris, Z. Dutton, and C.H. Behroozi, Nature (London) **397**, 594 (1999).
[40] S. Inouye, R.F. Löw, S. Gupta, T. Pfau, A. Görlitz, T.L. Gustavson, D.E. Pritchard, and W. Ketterle, Phys. Rev. Lett. **85**, 4225 (2000).
[41] P. Öhberg, Phys. Rev. A **66**, 021603 (2002).
[42] M. Artoni and I. Carusotto, Phys. Rev. A **67**, 011602 (2003).
[43] A. Aspect, E. Arimondo, R. Kaiser, N. Vansteenkiste, and C. Cohen-Tannoudji, Phys. Rev. Lett. **61**, 826 (1988).

[44] F. Brennecke, S. Ritter, T. Donner, T. Esslinger, Science **322**, 235 (2008).

[45] M.R. Matthews, D.S. Hall, D.S. Jin, J.R. Ensher, C.E. Wieman, E.A. Cornell, F. Dalfovo, C. Minniti, S. Stringari, Phys. Rev. Lett. **81**, 243 (1998).

[46] D.S. Hall, M.R. Matthews, J.R. Ensher, C.E. Wieman, and E.A. Cornell, Phys. Rev. Lett. **81**, 1539 (1998); D.S. Hall, M.R. Matthews, C.E. Wieman, and E.A. Cornell, Phys. Rev. Lett. **81**, 1543 (1998).

[47] Eqs.(61,62,64,66,68) have been obtained from the operatorial form of (56), where the atomic field operators have already been reduced to 2D. This is an approximation. The exact mean intensity of the light field involves the expectation value of products of $\hat\phi_{3D}$ and $\hat\phi_{3D}^\dagger$ that are not normally ordered, and one has to put the atomic field operators in normal order before the 2D reduction. In the operatorial form of (56), this amounts to replacing $\mathbf{k}_c\cdot[\mathbf{j}+\frac{\hbar}{2im}\nabla n]$ with $(\mathbf{k}_c-\mathbf{k}_p)\cdot\mathbf{J}$, where $\mathbf{J}(x,y)=\int_{-\infty}^{+\infty}dz\frac{\hbar}{im}\hat\phi_{3D}^\dagger(x,y,z)\nabla\hat\phi_{3D}(x,y,z)$. Then one finds additive corrections to the above mentioned equations. For example, for $k_p\simeq k_c$, in Eq.(66) one has to add to the expression $\frac{k_BT\rho(\mathbf{r}_0)}{m}[\cos^2\phi_{\rm sc}+f_n\sin^2\phi_{\rm sc}]$ the correction $\hbar\omega_z\rho(\mathbf{r}_0)/(2m)$. This correction, corresponding to spontenous emission due to the motional coupling between $|NC\rangle$ and $|C\rangle$ along z, is a flat function of $\phi_{\rm sc}$, that can thus be distinguished experimentally from the the relevant $f_n\sin^2\phi_{\rm sc}$ component.

[48] J. J. Hope and J. D. Close, Phys. Rev. Lett. **93**, 180402 (2004).

[49] J.M. Vogels, C.C. Tsai, R.S. Freeland, S.J.J.M.F. Kokkelmans, B.J. Verhaar, and D.J. Heinzen, Phys. Rev. A **56**, R1067 (1997).

[50] For a review on atomic collisions, see e.g. C. Chin, R. Grimm, P. Julienne and E. Tiesinga, Rev. Mod. Phys. **82**, 1225 (2010) and references therein.

[51] F. Gerbier, Y. Castin, Phys. Rev. A **82**, 013615 (2010).

[52] We used the fact that, for a generic function F satisfying $F[-(\mathbf{k}+\mathbf{q})]=F(\mathbf{k})$ for all $\mathbf{k}$, one has $\sum_{\mathbf{k}\neq\mathbf{0},-\mathbf{q};k_y>0}F(\mathbf{k})=\sum_{\mathbf{k}\neq\mathbf{0},-\mathbf{q};k_y<0}F(\mathbf{k})$.

[53] Experimentally, thermal equilibrium in the rotating frame is not always granted. Most likely, it was not achieved in the experiments of [11] where the vortex lattices did not nucleate at the expected Landau critical rotation frequency, but rather at a higher rotation frequencies when a dynamical instability of the condensate was triggered [12]. This picture was confirmed by numerical simulations [13].

[54] Note that the current operator $\mathbf{j}(\mathbf{r})$ has to be distinguished from the physical current $\mathbf{j}_{\rm phys}=\mathbf{j}-\mathbf{A}\hat\phi^\dagger\hat\phi/m$ corresponding to mass transport.

[55] In principle, one should remind that the Gaussian profiles are at angles $O(q/k_p)$ with respect to the $z=0$ plane. However, the resulting z-dependence of $\Omega_p^\pm$ can be safely neglected as it occurs on a length-scale $O(w\,k_p/q)$ much larger than the spatial extension $a_{\rm ho}^z$ of the atomic cloud along z.

[56] Note that the $-\int\mathbf{j}\cdot\mathbf{A}$ gauge Hamiltonian is equivalent to the first-quantized form $-\sum_{j=1}^N[\mathbf{p}_j\cdot\mathbf{A}(\mathbf{r}_j)+\mathbf{A}(\mathbf{r}_j)\cdot\mathbf{p}_j]/2m$ where N is the particle number. Differently from [16], our scalar potential W includes the A^2 term.

[57] For the choice (23), to zeroth order in q and $1/w$, W actually vanishes to all order in Ω_p/Ω_c. To order q^2, it does not vanish and scales as $-\hbar^2q^2|\Omega_p/\Omega_c|^2/(4m)$, which gives for the parameters of Table I a negligible contribution $\Delta E_W/\Delta E_2\approx 10^{-3}/f_n$ to the deposited energy scheme.

[58] The spatio-temporal dependence of $g_{3D}(\mathbf{r})=g_{aa}+\Delta g(\mathbf{r})\simeq g_{aa}+2(g_{ab}-g_{aa})\,|\Omega_p(\mathbf{r})/\Omega_c|^2$ is responsible for spurious excitation of the gas via two different effects that can be captured by a Bogoliubov treatment. (i) An effective potential appears of the form $\Delta V_g(\mathbf{r})=\rho_{3D}\,\Delta g(\mathbf{r})$: its modulated part at $\pm\mathbf{q}$ is able to excite phonons. (ii) The modulation of interaction constant is able to excite pairs of phonons by a parametric down-conversion effect [24]. For suitable atomic species such that $g_{aa}\simeq g_{ab}$ (in particular Rb atoms), the spurious deposited energy turns out to be smaller than the quantity ΔE_2 to be measured (see Appendix D for the analysis of one of the contributions.

[59] More precisely, $\ln\zeta=4G/\pi-2\ln 2$, G being the Catalan constant $G\simeq 0.91596\ldots$

[60] The discrete Laplacian Δ admits the plane waves $e^{i\mathbf{k}\cdot\mathbf{r}}$ as eigenmodes on the lattice with eigenvalue $\hbar^2k^2/2m$. In practice a Fast Fourier Transform is used to evaluate the action of the Laplacian on the field Ψ.

[61] To be complete, we have also performed simulations above the critical temperature, at $T/T_d=0.18$ (not shown). Since there is no superfluid phononic branch, we expect that lower values of $q\xi$ are requested to reach the $q\to 0$ limit. In the numerics, we indeed find that $q\xi=1/4$, with $\gamma/(c_sq)=0.2$ and 0.1, is requested to approach the value of f_n with the same relative error as in Fig.4. In this above T_c case, it is tempting to use the ideal gas model. Then for $\hbar^2q^2/m\ll k_BT\ll k_BT_d$, one obtains for the quantum gas $\lim_{\gamma\to 0}(f_n^{\rm eff}-f_n)\simeq(2T/T_d)[1-\mathrm{atanh}\,X/X]$ with $X=\epsilon/(4+\epsilon^2)^{1/2}$, $\epsilon^2=\hbar^2q^2/(2m|\mu|)$ and the chemical potential $\mu\simeq-k_BT\exp(-T_d/T)$. However this seems to give a significantly smaller error than in the numerics.

[62] A sufficient condition is that the uncertainty in the initial total energy is $\ll\hbar\gamma$.

[63] As a consequence of the continuity equation, the fluctuations of the density and of the longitudinal current are related by $\omega n_{\mathbf{q}}=\mathbf{q}\cdot\mathbf{j}_{\mathbf{q}}$. For small wavevectors, fluctuations are mostly sound-like with $\omega\simeq c_s\,q$. Inserting this result into the continuity equation, one finds that $\hbar q n_{\mathbf{q}}/2m\ll j_{L,\mathbf{q}}$ if $q\xi/2\ll 1$.

[64] Note that, for the second choice of laser configuration to come, atoms with a $J=1\to J'=1$ transition and a large fine structure are quite favorable, because the spurious lightshift U_p is strongly suppressed. Also, since $|a\rangle=|J=1,m=-1\rangle$ and $|b\rangle=|J=1,m=0\rangle$, one finds $g_{aa}=g_{ab}$ from rotational symmetry arguments [22, 23]. A potential problem to take care of is the partial inelastic nature of the bb collisions.

[65] This choice for $|e\rangle$ increases the branching ratio B of Eq.(58) by a factor 3 with respect to the choice $|F'=1,m_{F'}=-1\rangle$.

[66] We have checked that the contribution to $\langle C|-\partial_t|NC\rangle$ of the switch-off function $f(t)$ in Ω_p (that was not included in (52)) gives a negligible correction to the estimate of the fluorescence rate.

[67] Any two-photon Raman coupling of the $|NC\rangle$ state to $|c\rangle$ via the excited state sublevel $|e\rangle$ vanishes thanks to the destructive interference of the two paths $|a\rangle\to|e\rangle\to|c\rangle$

and $|b\rangle \to |e\rangle \to |c\rangle$.

[68] At the lowest order in Ω_p/Ω_c, the effect of a non-zero $g_{aa} - g_{ab}$ is to introduce a smooth polarization profile $\mathcal{P}_p = -[4|d_{ae}|^2/\hbar^2|\Omega_c|^2]\,(g_{aa} - g_{ab})\,n_{3D}^2\,\mathcal{E}_p$. As the corresponding phase shift does not depend on Ω_p/Ω_c, it can be isolated in the experiment. The contribution of higher order terms $O[|\Omega_p/\Omega_c|^3]$ have a non-trivial spatial structure and may interfere with the signal to be measured. Their relative value as compared to $\Delta\phi_2$ is however a factor roughly $\frac{g_{aa}-g_{ab}}{g_{aa}}\,\tilde{g}\,(\rho\lambda_c^2)/(2\pi^2 f_n)$ weaker.